WETTING BEHAVIOR AND SURFACE POTENTIAL CHARACTERISTICS OF HUMAN HAIR

A Thesis
Presented in Partial Fulfillment of the Requirements for
the Degree of Master of Science in the
Graduate School of The Ohio State University

By

Richard A. Lodge, B.S.

****

The Ohio State University

2007

Master's Examination Committee

Professor Bharat Bhushan, Advisor

Professor Vish Subramaniam

Approved by

_____

Advisor

Mechanical Engineering Graduate Program

ABSTRACT

The ways in which common hair care products, such as conditioner, deposit onto hair and change hair properties are of interest in beauty care science, since these properties are closely tied to product performance. In this thesis, a variety of studies are conducted to advance the current characterization of human hair. Tapping mode atomic force microscopy (AFM) is used to generate surface height maps of hair, which are then compared to maps generated using contact mode AFM. Contact mode has been used in the past and has the potential of damaging small surface features, while tapping mode does not. The frequency spectra of both data sets are also compared. This comparison is made to determine the most appropriate method for imaging compliant biological samples that may be subject to damage from interaction with the AFM tip during contact mode. Additionally, force calibration mode of AFM is used to obtain the local conditioner thickness distribution and adhesive force mapping of various hair surfaces. The conditioner thickness is extracted by measuring the forces on the AFM tip as it approaches, contacts, and pushes through the conditioner layer. Because the interaction of hair with skin is one of the most common in the real world, and clean skin is hydrophobic, a Si_3N_4 tip is coated with Z-TETRAOL to create a hydrophobic tip to measure friction and adhesion. These values are compared with those measured with the more common, hydrophilic tips.

To further the study on the effect of contact angle, the wettability of human hair is studied by using the Wilhelmy balance method to measure dynamic contact angle of hair with water. The method uses a microbalance to measure the force exerted on a single fiber when it is immersed into the wetting liquid of interest. This measured force is related to the wetting force of the liquid on the fiber, and the dynamic contact angle can be calculated. Hair samples were measured dry, and then also allowed to soak in water before being measured to determine if a wet environment affects the wetting properties of the hair surface. Additionally, hairs from subjects of different ethnicities are measured and compared. Further, the mechanisms driving a significant directionality dependence are studied and discussed. The results are also used to explain tribological properties found in previous studies.

The final property of interest in this thesis is the surface potential of human hair. Surface charge of hair has a significant effect on manageability, feel, and appearance. For this reason, controlling charge buildup to improve these factors is an important issue in the commercial hair care industry. In this portion of the thesis the surface potential of human hair is measured using the Kelvin Probe method with an atomic force microscope (AFM). In the first part of this study, samples are mounted in conductive silver paint, and a DC voltage is applied through the sample puck. The surface potential is then measured as the applied voltage is changed. In the second part of the study, physical wear and triboelectric charging are investigated with the Kelvin probe technique. Physical wear has been shown to cause surface potential change in conductors and semiconductors, and it is of interest whether or not physical wear alone can cause a surface potential change on hair and other insulating materials.

It is known that interaction of hair with dissimilar materials, such as plastic combs, hands, and latex balloons, creates a charge on hair, and determining the mechanisms of this phenomenon is the purpose of this study. A variety of samples are worn with a diamond tip to investigate the effect of physical wear on surface potential. Additionally, hair samples are rubbed with latex to study the effect of triboelectric charging on the microscale. The surface potential is measured both prior to and after rubbing to observe how the surface charge changes.

Caucasian virgin (undamaged), chemically damaged, and mechanically damaged hair samples are studied to determine the effect of damaging treatments on surface charge properties. Samples treated with PDMS silicone conditioner as well as those treated with an amino silicone conditioner are also studied in some cases to determine the effect of conditioner treatment. Finally, hair samples from subjects of varying ethnicities are used to examine any differences in properties due to ethnicity.

ACKNOWLEDGMENTS

I would first like to thank my advisor, Professor Bharat Bhushan, for giving me the opportunity, resources, and support to be successful in his lab. I have learned a great deal from this experience both technically and personally, and the lessons I will take with me I'm sure will prove invaluable. I have gained a new perspective on engineering and on life that I would otherwise not have.

I would also like to thank Dr. Peter Torgerson, Dr. Rob Willicut, Dr. Matt Wagner, and Mr. Michael Mootz for their contributions. There is no doubt I would not have the in depth understanding of the science of hair care without their help. Their help and expertise has proven to be a great resource, and I could not have completed this work without it. I would also like to thank the Procter and Gamble Company for providing financial support needed for this work.

I would especially like to thank my colleagues here at NLIM. Specifically I would like to recognize Dr. Zhenhua Tao, Dr. Michael Cichomski, and Dr. Manual Palacio for spending time making samples for my work, as well as providing additional perspectives on technical issues. I would also like to thank my predecessor, Mr. Carmen LaTorre, for spending an immense amount of time teaching me the basics of atomic force microscopy and helping me to get started on this work. His

help and selflessness has proven to be a priceless gift that has made my success here possible.

Finally, I would like to thank my parents, Dick and Martha Lodge for their love and support. From them I have learned the importance of hard work and dedication, as well as having passion for and pride in my work. From an early age my dad has instilled in me the importance of the scientific method and logic in engineering work, and in life, which has proven to be an invaluable tool throughout my experience at NLIM. They have taught me to keep an open mind and to be creative and to have respect for others, and I can not thank them enough.

VITA

July 18, 1982	Born – Cincinnati, OH
2005	B.S. Mechanical Engineering, The Ohio State University
2005 – present	Graduate Research Associate, The Ohio State University

PUBLICATIONS

1. R.A. Lodge and B. Bhushan, "Surface characterization of human hair using tapping mode atomic force microscopy and measurement of conditioner thickness distribution", *J. Vac. Sci. Tech. A*, **24**, 1258-1269 (2006).

2. R.A. Lodge and B. Bhushan, " Wetting properties of human hair by means of dynamic contact angle measurement" *J. App. Poly. Sci.* **102**, 5255-5265 (2006).

3. R. A. Lodge and B. Bhushan, "Surface potential measurement of human hair using Kelvin probe microscopy", submitted for publication (2006).

4. R.A. Lodge and B. Bhushan, "Effect of physical wear and triboelectric interaction on surface charge as measured by Kelvin probe microscopy", submitted for publication (2006).

FIELDS OF STUDY

Major Field: Mechanical Engineering

TABLE OF CONTENTS

LIST OF FIGURES

LIST OF TABLES

CHAPTER 1

INTRODUCTION

The desire for products that improve the look and feel of hair has created a huge industry for hair care. The ways in which common hair care products, such as conditioner, deposit onto and change hair properties are of interest in beauty care science, since these properties are closely tied to product performance. Conditioner is one hair care product which is very commonly used by consumers. Conditioner thinly coats hair and can cause drastic changes in the surface properties of hair. The layer of conditioner creates a softer, smoother feel for the consumer and provides a protective coating on the hair surface for prevention of future damage. Conditioner consists of a gel network chassis (cationic surfactant, fatty alcohols and water) for superior wet feel and a combination of conditioning actives (silicones, fatty alcohols and cationic surfactant) for superior dry feel. Cationic surfactants are critical to the forming of the lamellar gel network in conditioner, and also act as a lubricant and static control agent, since their positive charge aids in counteracting the negative charge of the hair fibers. The cationic surfactants in the conditioners used in this study are quaternary amine-based surfactants. They have a low energy alkyl chain on one end of the molecule and relatively higher energy cationic group on the other. Fatty alcohols are used to lubricate and moisturize the hair surface, along with forming the gel network. Among

all the components of conditioner, silicones are the main source of lubrication for dry hair.

Fig. 1.1 shows the schematic structure of a human hair fiber and its various cellular structures (Feughelman, 1997; Morioka, 2005; Robbins, 1994; Zviak, 1986). Hair fiber (about 50-100 μm in diameter) consists of cuticle and cortex cells which run longitudinally along hair fiber. The cortex takes up the majority of hair fiber composition and the cuticle is the outermost region that protects the cortex. The cuticle consists of flat overlapping cells (scales). The cuticle cells are attached at the root end and they point forward toward the tip end of hair fiber, like tiles on a roof. Each cuticle cell is approximately 0.3 to 0.5 μm thick and the visible length of each cuticle cell is approximately 5 to 10 μm. The cuticle in human hair is generally 5 to 10 scales thick.

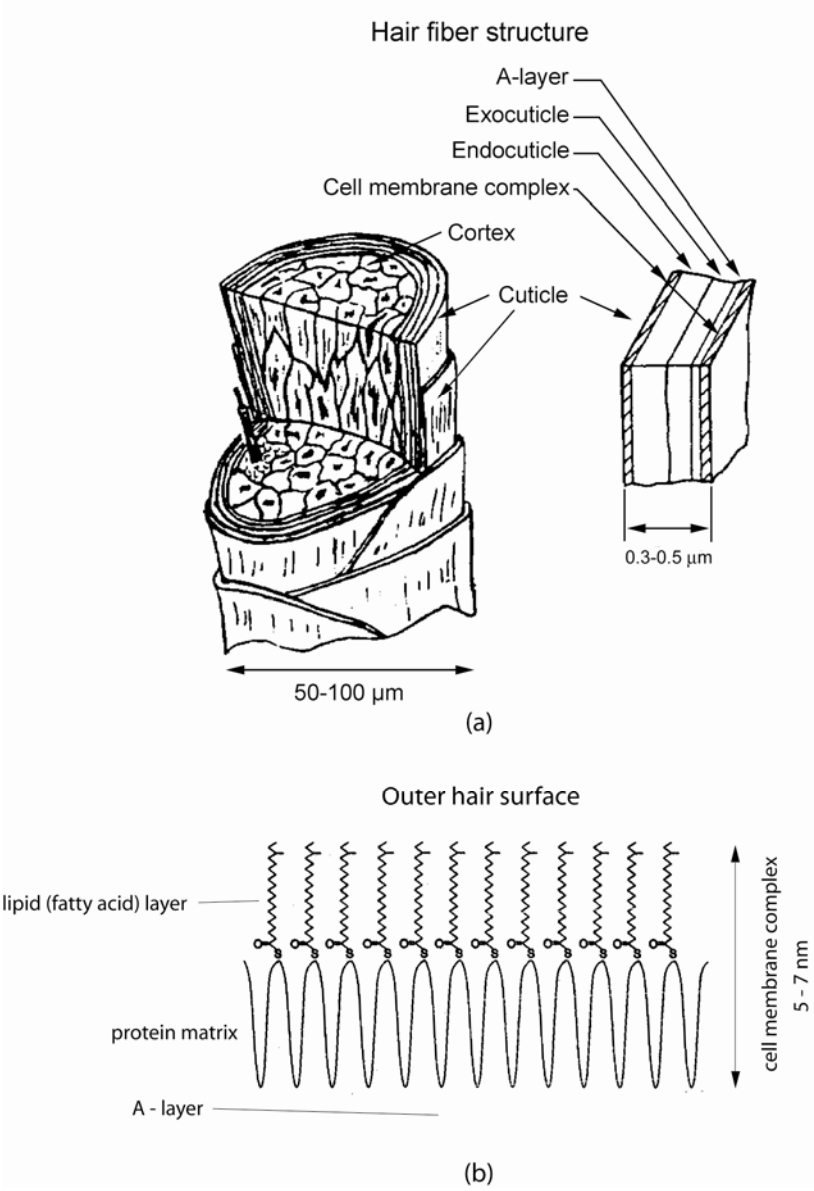

Figure 1.1 (a) Schematic structure of human hair.[Robbins, 1994] ; (b) Schematic of outermost surface of hair showing 18-MEA location [Negri and Cornell, 1993].

Each cuticle cell consists of various sublamellar layers: the A-layer, the exocuticle, the endocuticle, and the cell membrane complex. The cell membrane complex consists of a protein matrix and a lipid layer; see Fig. 1.1(b). The lipid layer consists of fatty acids, primarily 18-methyleicosanoic acid (18-MEA), which strongly

contributes to the hydrophobicity and lubricity of virgin hair. This fatty acid is intact in virgin hair, but is removed during chemical treatment, causing a slightly hydrophilic and less lubricious surface for chemically damaged hair (Kamath *et al.*, 1978; Negri and Cornell, 1993; Molina *et al.*, 2001; LaTorre and Bhushan, 2006a; LaTorre and Bhushan, 2006b; Lodge and Bhushan, 2006a; Lodge and Bhushan, 2006b). This is also the case for mechanically damaged hair, where the mechanical damage physically removes the top, hydrophobic layer of the hair.

Previous studies have reported mechanical and tribological properties of hair using atomic force microscopy (AFM) in so called contact mode using a Si_3N_4 tip (LaTorre and Bhushan, 2005a; LaTorre and Bhushan, 2005b). In this method the tip is in full contact with the hair sample and a constant normal load between tip and sample is maintained. This causes a significant lateral force to exist between tip and sample, and creates the potential for damage to the sample. Hair, like other biological samples in general, is rather compliant (Wei *et al*., 2005), and therefore tapping mode AFM is investigated as a more appropriate method for surface height imaging. In this method, the AFM tip lightly taps the sample surface at a constant amplitude to gather information on the height of the sample surface. In general, it is a much less destructive method, and results in a negligible lateral force between tip and sample.

Table 1.1 shows contact angles for various hairs, human skin, Si_3N_4, and Z-TETRAOL coating, and shows that Si_3N_4 is hydrophilic (contact angle ~ 35º) (LaTorre et al., 2006; Tao and Bhushan, 2006). This allows the possibility of

significant meniscus force contributions to friction and adhesion when using a Si_3N_4 tip in contact mode. One of the most important interactions in hair care science is that between hair and fingers.

	Contact angle (°)	Surface energy (N/m)
Human hair - virgin untreated	103[a] 100[b]	0.024[a] 0.028[b]
- damaged brown coloring blond coloring	60[b] 55[b]	0.038[b] 0.047[b]
PDMS (bulk)	105[c]	0.020[d]
Human skin - forehead - forearm - finger	55[e] 88[e] 84[f] 74[f] 58[g] (before soap-washing) 104[g] (after soap-washing)	0.043[e] 0.038[e] 0.029[f] 0.024[f] 0.027[g]
Si_3N_4 film	35[b]	0.047[i]
Z-TETRAOL Coating	97[j]	

[a] Molina et al. (2001)
[b] LaTorre et al. (2006)
[c] Bhushan and Burton (2005)
[d] Jalbert et al. (1993)
[e] Lerebour et al. (2000)
[f] Schott (1971)
[g] Ginn et al. (1968)
[i] Yanazawa (1984)
[j] Tao and Bhushan (2005)

Table 1.1 Contact angle and surface energy of relevant materials associated with nanotribological characterization of hair.

This is because shampoo and conditioner are applied with the fingers, and achieving a smooth feel when running one's fingers through one's hair is a

fundamental goal of conditioner. Untreated finger skin tends to be hydrophilic (contact angle ~ 74º) (Schott, 1971), while cleaned finger skin tends to be hydrophobic (contact angle ~ 104º) (Ginn *et al.*, 1968). For this reason, it is of interest to measure tribological properties with a hydrophobic tip in addition to the measurements previously taken with hydrophilic tips. To create a hydrophobic Si_3N_4 tip, a tip was coated with Z-TETRAOL as described by Tao and Bhushan (2006). The tip was dip coated in a Z-TETRAOL solution and baked to create a fully bonded Z-TETRAOL layer on the tip surface. This process raised the contact angle to near 97º.

Mapping conditioner thickness gives a clear picture of where conditioner deposits on the hair surface. Understanding how conditioner distributes and behaves on the hair surface is a critical insight into the mechanisms behind conditioner's interaction with hair. To obtain the local conditioner thickness distribution on various hair surfaces, force calibration plot measurements using an AFM are conducted. The conditioner thickness is extracted by measuring the forces on the AFM tip as it approaches, contacts, and pushes through the conditioner layer.

Both tapping mode and contact mode images are created, and their corresponding power spectrum density function plots (PSDFs) are compared. PSDF analysis gives a quantitative description of the size of surface features that are captured in both tapping mode and contact mode. This helps indicate any instances in which small surface features are deformed due to interaction with the AFM tip. Conditioner thickness and adhesive force maps are also generated using a Si tip. This helps generate a better understanding of how conditioner changes surface

properties of hair, and what alterations to conditioner composition may improve product performance. Also, coefficient of friction is measured and adhesive force maps generated using both coated and uncoated Si_3N_4 tips. The location of conditioner deposits, effect of location on surface properties, and mechanisms behind the deposition and trends observed in the data are all thoroughly discussed.

Another critical property in hair care science is the contact angle of hair with water. Due to the fact that water is prevalent in the air, and conditioner and other hair products are applied in a wet environment, the wetting properties of hair are of interest. It has also been shown that the contact angle of water on an AFM tip significantly affects the measured values of friction and adhesion using that tip (Lodge and Bhushan, 2006), as does the contact angle of water on the measured surface itself. Similarly, the way in which damage and conditioner treatment affects the wetting properties of hair is also important in understanding the tribological properties of hair. However, the size and geometry of a hair fiber make static contact angle measurement with a goniometer difficult and unreliable. For this reason, dynamic contact angles are measured using the Wilhelmy balance method (Wilhelmy, 1863) in which a microbalance is used to measure the wetting force. This method is often used to measure wetting properties of thin fibers (Hoecker and Karger-Kocsis, 1996). Ecke *et al.* (1999) used an atomic force microscope (AFM) to study wetting of individual particles. AFM has also more recently been used to measure the dynamic contact angle of carbon nanotubes (Barber *et al.*, 2005). In addition, the

Wilhelmy balance technique has been employed to study hair fibers (Kamath *et al.* 1978; Molina *et al.*, 2001), although the effect of conditioner treatment has not been previously studied.

In the Wilhelmy balance method a single fiber is suspended from a microbalance. A beaker of the wetting liquid sits on a stage below the fiber sample to be measured. The liquid moves toward the fiber at a constant velocity (advancing mode) until the sample contacts the liquid surface. The liquid then continues in the same direction, submerging the fiber to a specified depth (1 mm in this study), and then moves away from the fiber (receding mode) until the fiber is completely out of the wetting liquid. The force exerted on the hair fiber is related to the contact angle of the fiber surface.

The final property of interest in this thesis is the surface potential of hair. Electrostatic charge on hair significantly affects look, feel, and manageability. To measure surface potential, Kelvin probe microscopy is employed. Kelvin probe has been used in a variety of applications to measure surface potential. Because of the sensitive nature of silicon to charge buildup and subsequent discharge which can damage small silicon parts, surface potential measurement has been of interest in the semiconductor industry. Doping has been used to increase conductivity and ability to dissipate charge safely, and thus the Kelvin probe method is useful for studying these issues (Schroder, 2006). The technique has also been used successfully to detect wear precursors from wear at very low load using AFM based Kelvin probe methods (DeVecchio and Bhushan, 1998; Bhushan and Goldade, 2000a, 2000b). In these studies it has been shown that physical wear, even at the very early stages of wear,

creates a significant change in surface potential. However, the results have only been proven for highly conducting samples and it is not clear whether physical wear on insulating samples could be responsible for a change in surface charge. This distinction from previous results is critical because human hair is an insulating material.

Conditioner is known to affect the surface potential characteristics of hair, and understanding this behavior on the small scale is of great interest. Similarly, the way in which various damaging treatments affect the measured surface potential of a hair will provide a new way to characterize the degree of damage. Because surface potential of human hair is of such interest, Kelvin probe may provide great insight into the mechanisms behind electrostatic behavior of hair. Similar studies have been conducted previously, but all measurement of surface potential has been qualitative or on the macroscale (Barber and Posner, 1958; Jachowicz *et al.*, 1985; Lunn and Evans, 1977; Mills *et al*., 1956). This thesis seeks to quantify those measurements while observing charge distribution on the microscale, and more importantly to detail the mechanisms behind surface potential change.

It is obvious that during combing and running the hands through one's hair that physical damage is likely to occur. These actions also tend to create an electrostatic charge on the hair, and it is of interest whether or not the physical wear and the electrostatic charge are related, or if charge by other mechanism has been created, as has been shown in previous studies as mentioned above. Therefore, the effects of physical wear on surface potential for both conducting and insulating samples are investigated to clarify the mechanism behind the behavior. Further,

electrostatic charging of hair is studied by charging the hair with latex, a material that is known to create a static charge on hair. The presence of this static charge in the real world is a major problem concerning hair manageability, so understanding the mechanisms behind charge buildup, and how to control it, is thus a focal point in designing effective hair care products such as conditioner.

CHAPTER 2

EXPERIMENTAL TECHNIQUES

A commercial AFM system (MultiMode Nanoscope IIIa, Veeco, Santa Barbara, CA) was used in ambient conditions (22 ± 1 °C, 50 ± 5 % relative humidity) for all AFM measurements, except for those specifically stated to have occurred in different humidity conditions. Contact mode images were taken using Si_3N_4 probes of 30-50 nm tip radius, at a normal load of 4-5 nN. Tapping mode images were made using Si probes with 10 nm tip radius. The cantilever was oscillated at its resonant frequency at an amplitude 90% of the amplitude in free air during imaging. Figure 2.1 shows a schematic diagram of the AFM.

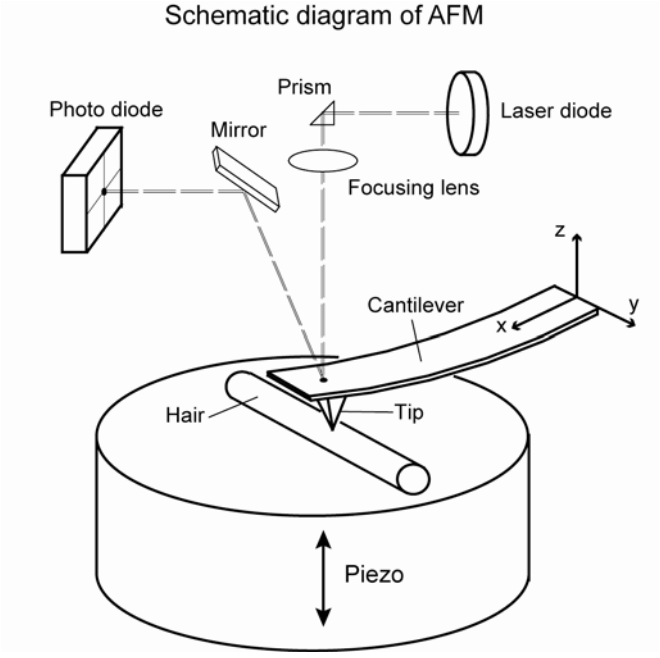

Figure 2.1 Schematic diagram of atomic force microscope (AFM).

In contact mode, the tip scans over the sample in full contact with the sample, at a constant normal load. While this allows for measurement of friction and adhesive forces, it also introduces the possibility for localized deformation of soft samples. In tapping mode, the tip is oscillated near its resonant frequency, and only lightly taps the sample surface. The control system seeks to maintain constant amplitude of these oscillations in this method. A schematic of these different modes is shown in Figure 2.2.

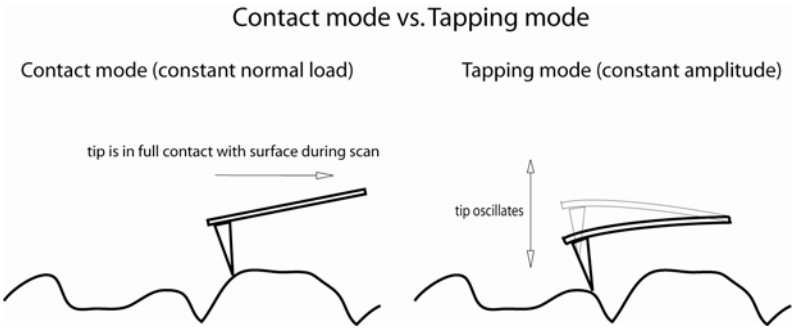

Figure 2.2 Schematic of contact mode and tapping mode AFM operation. Tip remains in full contact throughout scan in contact mode, while in tapping mode the tip only lightly taps the sample surface as it scans.

As tapping mode taps the surface, the lateral forces between sample and tip are reduced to near zero. This prevents any sample deformation due to the lateral tip interaction, and is generally capable of capturing more high frequency data from the sample surface (Bhushan *et al.*, 1997). The contrast between these two operating modes is shown in Figure 2.2. Both microscope modes are employed in this thesis.

2.1 Friction, adhesion, and conditioner thickness measurements

Friction force was measured based on a method by Bhushan (1999, 2002). Coefficient of friction values reported in this study were taken along the length of the hair shaft, away from cuticle edges. Values taken perpendicular to the hair shaft were found to display no significant difference to those taken along the length of the shaft. Therefore, measurements were made along the length of the shaft due to the greater simplicity as a result of the geometry of the hair. The normal load was varied from approximately 4 nN to 40 nN, roughly in increments of 5 nN, and friction force was measured at each normal load. The friction force was plotted as a function of normal load, and the average coefficient of friction was taken to be the slope of the line fit to this data.

To measure adhesion, the force calibration plot method was used. In the force calibration plot technique, the AFM tip is brought into contact with the sample by extending the piezo vertically (from point A to point E), then retracting the piezo to separate the tip from the sample (from point E to point H, then back to point A) as shown in Figure 2.3(a). The method is described in detail by Bhushan (1999a, 1999b, 2002, 2004).

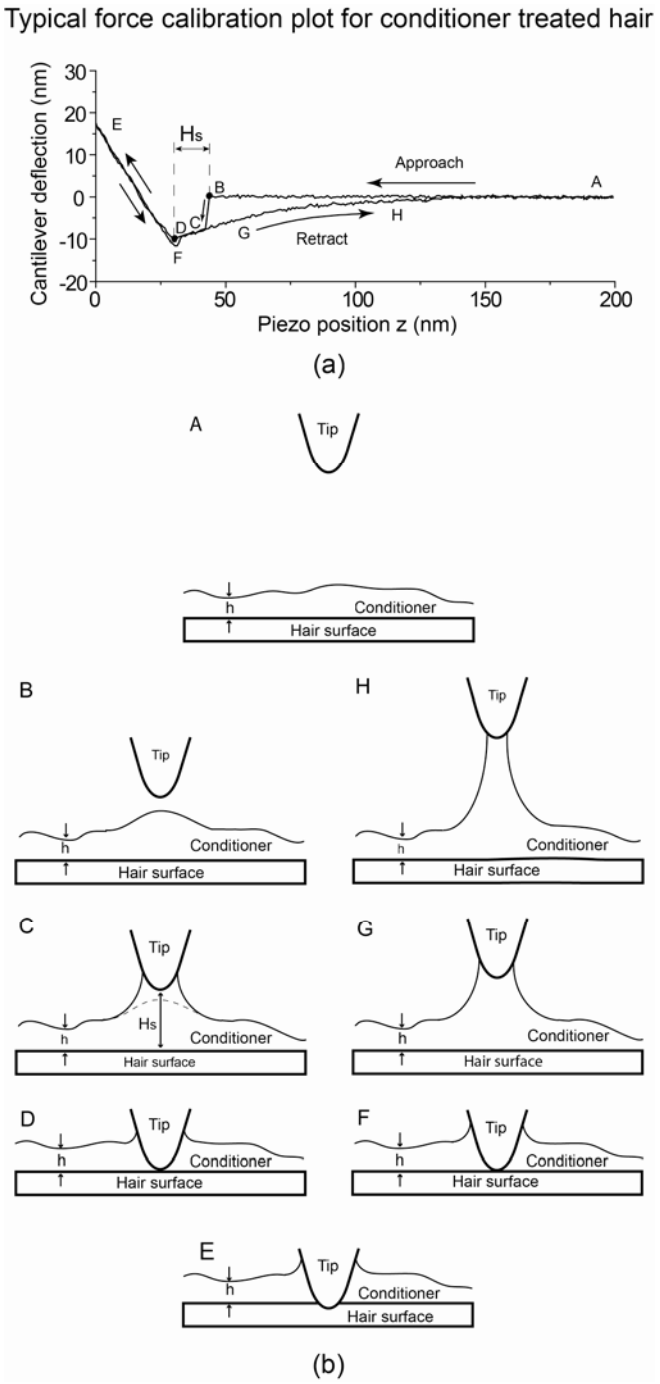

Figure 2.3 (a) A typical force calibration plot for commercial conditioner treated (3 cycles) hair. Snap-in distance, Hs, is a measure of film thickness on sample surface. ; (b) Schematic diagrams of the AFM tip, conditioner and hair surface at different tip sample separations as labeled in 2.3(a).

The force calibration plot allows measurement of the deflection of the cantilever as a function of the piezo position at a distinct point on the sample surface. Fig. 2.3(a) shows a typical force calibration plot curve for commercial conditioner treated hair. From this plot, the conditioner thickness and adhesive force can be extracted. The snap-in distance H_s, which is proportional to the real film thickness, is the horizontal distance between point B and point D; and the adhesive force F_a (on retract curve), which is the force needed to pull the sample away from the tip and is the sum of van der Waals force F_{vdw} mediated by adsorbed water or conditioner layer and the meniscus force F_m due to Laplace pressure ($F_a = F_{vdw} + F_m$), can be calculated from the force calibration plot by multiplying the spring constant with the vertical distance between point B and point F.

The meniscus force F_m is given by

$$F_m = 2\pi R\gamma(1+\cos\theta) \qquad \text{Eq. 2.1}$$

where R is the tip radius, γ is the surface tension of the conditioner, and θ is the contact angle between the tip and conditioner. The interaction between tip and sample is shown more closely in Figure 2.3(b). As can be seen from this figure, there may be some controversy between whether point B or point C is the more appropriate point to measure from. Point B is the point just before the tip and film layer come in contact. At point C, a meniscus bridge has formed between tip and sample, and they are already in contact. Because the depth at which the tip has already penetrated into the film layer at point C is not known, point B is used in this work. It is obvious that point B will overestimate the film thickness. From this study it is determined that the film thickness is overestimated approximately 1-2 nm.

Consequently, by taking a force calibration plot at discrete sampling intervals over an entire scan area, conditioner thickness, and adhesive force maps can be created to display the distribution and variation over the surface. In this study, the force curves were collected at the same maximum cantilever deflection (relative trigger mode), at each point at 64 × 64 array (total 4096 measurement points) with each force curve sampled at 64 points over a scan area of 2 × 2 μm^2 for all hair samples. A custom program coded in Matlab was used to calculate and display conditioner thickness and adhesive force maps.

Friction force was measured with a Si_3N_4 tip on a flexible cantilever of spring constant 0.06 N/m to minimize damage to the sample. Adhesive force maps taken with the Si_3N_4 tip were done with a cantilever of stiffness 0.58 N/m. This cantilever was chosen because large adhesive forces were expected, and the more flexible cantilever was unable to measure forces this high. Conditioner thickness measurements were made with FESP (force modulation etched Si probe) tips (100 nm radius[1], spring constant of 5 N/m), using the force calibration plot technique ("force-volume mode" of the nanoscope software). It should be noted that adhesive force maps were created using both the aforementioned Si tip during conditioner thickness measurement and the aforementioned Si_3N_4 tip. These different tips were chosen for the reasons described above, as well as to aid in comparison with results reported from previous studies. The results of this study show that using a different type of tip results in different adhesive forces as measured. This is due to the difference in

[1] Si tip radius is initially 10-20 nm. Because Si is brittle, when engaged in contact mode, tip will break and dull significantly. Radius measured after measurement was found to be near 100 nm.

material and geometry of the tips. It should be understood that the adhesive force results from two different types of tip should not be compared with one another, and should only be compared with results obtained using the same type of tip.

2.2 Dynamic contact angle measurements

To measure dynamic contact angle, the Wilhelmy balance method was used. In the Wilhelmy balance method a single fiber is suspended from a microbalance, shown in Fig. 2.4.

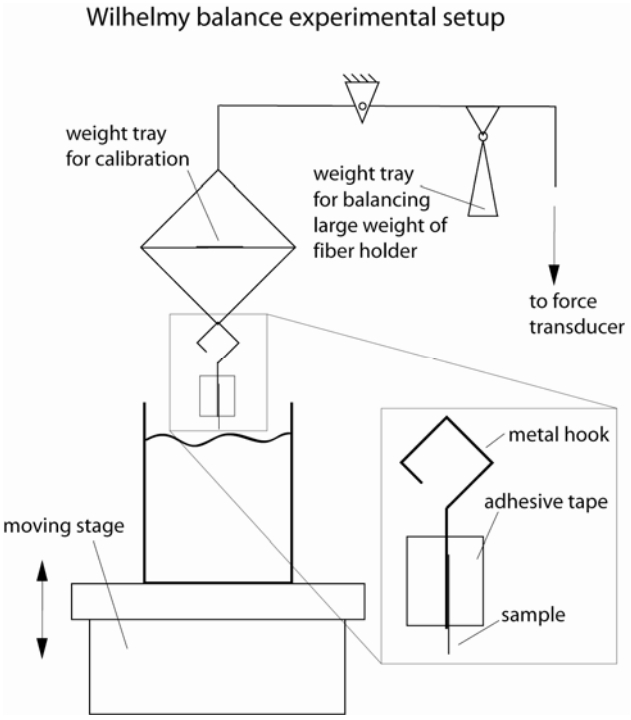

Figure 2.4 Schematic diagram of Wilhelmy balance technique measurement setup, and zoomed view of sample mounting.

A beaker of the wetting liquid sits on a stage below the fiber sample to be measured. The liquid moves toward the fiber at a constant velocity (advancing mode) until the sample contacts the liquid surface. The liquid then continues in the same

direction, submerging the fiber to a specified depth (1 mm in this study), and then moves away from the fiber (receding mode) until the fiber is completely out of the wetting liquid. The force exerted on the hair fiber is related to the contact angle of the fiber surface by the following equation:

$$F = \gamma P \cos\theta + W - \rho g y A \qquad \text{Eq. 2.2}$$

F = measured force

γ = surface tension of wetting liquid

P = wetted perimeter of fiber at liquid/air interface

θ = contact angle of fiber surface

W = weight of fiber

ρ = density of wetting liquid

y = immersion depth

A = cross sectional area of fiber

The first term in Eq. 2.2 is the wetting force acting on the fiber, the second is the weight of the fiber, and the third represents the buoyancy force on the fiber. The weight of the fiber is tared prior to measurement, and the buoyancy is neglected as it is several orders of magnitude smaller than the measured force. With the preceding assumptions, the relation reduces to:

$$F = \gamma P \cos\theta \qquad \text{Eq. 2.2(a)}$$

A Cahn DCA-322 Dynamic Contact Angle Analyzer was used in this study. This device employs a microbalance to measure the wetting force as described above and shown in Figure 2.4. Tests were carried out in a 50-60% relative humidity and 22

$\pm$ 1 ºC environment. Samples were exposed to this environment for a minimum of 30 minutes prior to measurement to allow them to equilibrate. All water contact angle measurements were taken using deionized water.

As previously mentioned, the force measured by the microbalance is related to the contact angle of the sample surface by Eq. 2.2(a). However, this relation makes assumptions which must be discussed. The fiber is assumed to be normal to the liquid surface, but due to the natural curl of most hairs, mounting the hair exactly normal to the liquid surface is nearly impossible. An off-normal fiber has the effect of producing a larger actual wetted perimeter than one calculated using the nominal diameter of the hair. To deal with this issue, the wetting perimeter is measured by employing the same technique with a liquid of known contact angle. In this study, octane was used, as it is believed to completely wet the solid surface due to its low surface tension and apolarity, and thus a contact angle of zero is assumed. The octane used in this study was reagent grade (95% pure, minimum) octane supplied by Fisher Scientific. This technique is employed with a similar liquid, decane, by Molina[7] *et al*. Error analysis indicates that even if these liquids do not have a contact angle of zero, the error that results is acceptable. The largest error would arise for measured contact angle closest to 45º. For this study, this corresponds to an angle of around 70º, with a cosine of 0.342. If the actual contact angle of this sample with octane is 30º, the actual contact angle with water is 66.7º, giving slightly less than 5% error in the calculated contact angle. The other extreme found in this study, 103º (contact angle of virgin hair with water), gives an error of only 2% for the conditions stated above. This error is considered acceptable and thus measuring perimeter by immersion in

octane is used throughout this portion of the research. With the only unknown left in Eq. 2.2(a) being the wetted perimeter, this value can be calculated. In this study hair fibers were tested in water first, then in octane to obtain perimeter data. It should be noted that it is also possible that an off-normal fiber will flex during immersion bringing it normal to the liquid surface, thus negating any issues that arise with an off-normal fiber. Though this behavior was not monitored and can not be confirmed, the use of octane to measure perimeter and the possibility of fiber flexure make off-normal effects negligible.

Similarly, if the force is large enough to cause the hair fiber to buckle, an off-normal effect will exist. Only hydrophobic fibers will have this problem as the wetting force will be compressive, whereas it is tensile for hydrophilic fibers. The use of octane to alleviate this issue is not sufficient since the buckling in water does not necessarily imply buckling in octane, thus the wetted perimeter measured in octane would be different than in water. Therefore the experiment was designed to ensure buckling did not occur. The buckling issue is analyzed by using the Euler buckling equation[13]:

$$P_{cr} = \pi^2 EI/L_e^2 \qquad \text{Eq. 2.3}$$

P_{cr} = critical buckling load

E = tensile elastic modulus of hair fiber

I = area moment of inertia of circular cross section

L_e = unsupported length of hair

To design the experiment so buckling does not occur, a maximum unsupported fiber length was calculated. The modulus of elasticity used was 3 GPa, which is a

conservative estimate based on the 3.89 GPa reported by Robbins[3]. The maximum compressive force measured in this study was approximately 4 μN. Finally, a conservative fiber radius of 15 μm was used to calculate the moment of inertia, as this is the minimum radius observed. Using these values the critical unsupported fiber length at which buckling would occur is approximately 17 mm. To prevent buckling and to obtain the straightest fiber possible, an unsupported length of 5 mm or less was used.

Additionally, significant hysteresis is observed for the advancing and receding modes. Fig. 2.5 shows a typical force plot for virgin hair.

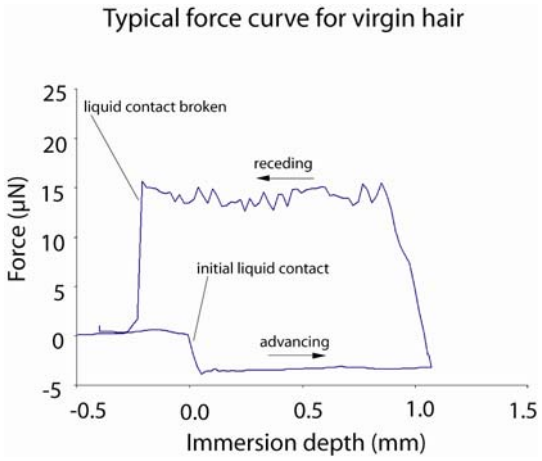

Figure 2.5 A typical force curve for virgin hair showing advancing and receding regions.

It should be noted that a negative value of force indicates an upward (compressive) force on the fiber, indicating the fiber is hydrophobic. A positive force indicates a downward (tensile) force on the fiber, indicating it is hydrophilic. The hysteresis is quite obvious here as the advancing mode shows a much lower force than does the receding mode. The reason for this is shown in the cartoon of Fig. 2.6.

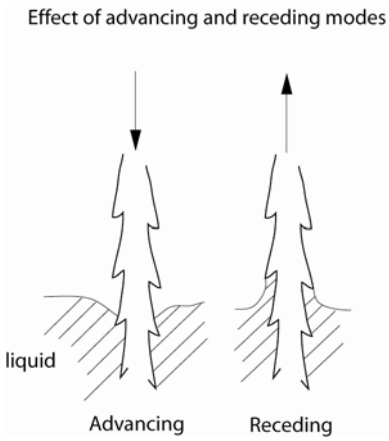

Figure 2.6 Schematic of liquid/hair interaction during measurement process. Advancing direction correlates to contact angle values of the hair surface away from the scale edge. Receding direction correlates to values that are heavily influenced by scale edge contributions. Receding direction also influenced by liquid properties (Lam, 2001).

During advancing mode, the wetted perimeter is that of the general surface of the cuticle scales, away from the scale edges. During receding mode, the opposite is true, and the wetted perimeter tends to exist at the scale edges. Due to the fact that the scale edges are more prone to mechanical damage from handling, they are more likely to have the hydrophobic top layer removed exposing the hydrophilic underlayers. Likewise, the scale edge surfaces are very far from normal to the liquid surface, often times they are almost parallel, whereas the hair surface away from the edges is very close to normal. Because the fiber surface must be normal to the liquid surface to employ the Wilhelmy technique, measurements which are heavily influenced by the scale edges are not accurate and are therefore not used in this study. Similar arguments for this hysteresis are given by Kamath[5] *et al.* and Molina[7] *et al*. Additionally, a study by Lam[14] *et al.* suggests that receding contact angles are

influenced by wetting liquid properties, and are not a function of the solid surface alone. For these reasons, only advancing contact angles are used as they more accurately reflect the wetting properties of the hair surface.

The following values for surface tension were used[15]:

$$\gamma_{water} = 72.2 \text{ dyne/cm}$$

$$\gamma_{octane} = 22.0 \text{ dyne/cm}$$

2.3 Surface potential measurements

All surface potential measurements were taken with a MultiMode atomic force microscope equipped with Extender Electronics module (Veeco Instruments). The Extender allows for surface potential measurements to be taken. Surface potential measurement is conducted using a two pass method. In the first pass, surface topography is measured using the standard AFM tapping mode. In the second pass, the tip is scanned over the previously measured topography at a specified distance above the surface. In this study that distance is 10 nm. A schematic of both passes is shown in Fig. 2.7.

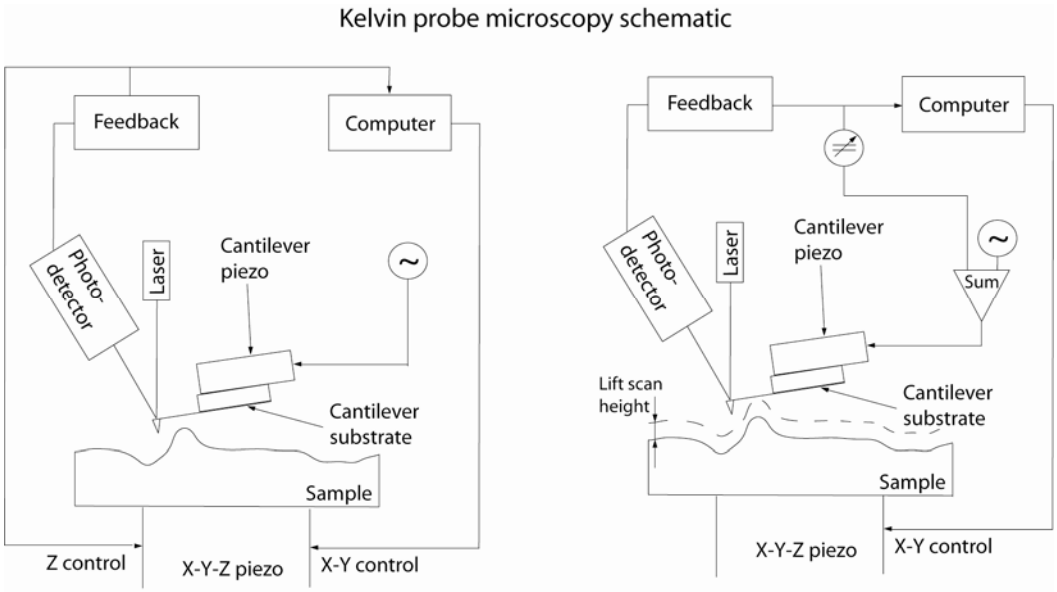

Figure 2.7 Schematic of first pass of Kelvin probe technique measuring surface height [Bhushan and Goldade, 2000a], and second pass measuring surface potential [Bhushan and Goldade, 2000a].

In the second pass the piezo normally oscillating the tip in tapping mode is turned off. Instead an oscillating voltage is applied directly to the conducting tip which generates an oscillating electrostatic force. The oscillating force has amplitude described by the following equation:

$$F = dC/dz\ v_{dc}\ v_{ac} \qquad \text{Eq. 2.4}$$

dC/dz – vertical derivative of tip-sample capacitance

v_{dc} – dc voltage difference between tip and sample

v_{ac} – amplitude of oscillating voltage applied to tip

To measure the surface potential, a dc voltage is applied to the tip until v_{dc} is equal to zero, giving zero oscillating force amplitude. Thus the surface potential at that point will equal the dc voltage applied to the tip to give zero oscillating force amplitude. In

this study Veeco probes MESP (Co/Cr coated Si) and SCM-PIT (Pt/Ir coated silicon) were used as the probe must be conductive to employ the Kelvin method. MESP tips were used for experiments employing the external voltage source and SCM-PIT were used for wear and latex rubbing experiments. Kelvin probe parameters were optimized using the scheme presented by Jacobs *et al.* (1998). To do this, an external function generator was used to apply a square wave to the sample. Jumper settings on the microscope to apply external voltage are shown in Fig. 2.8. These settings were used for optimization and for applied potential experiments.

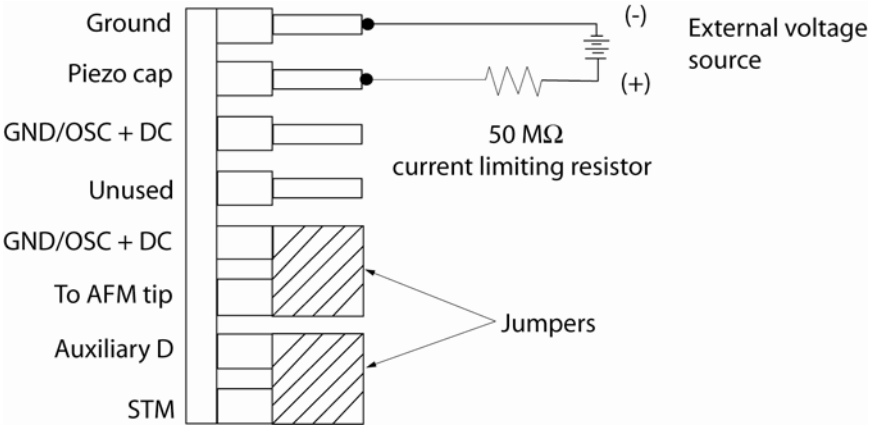

Figure 2.8 Jumper configuration and resulting electrical circuit setup during optimization procedure [Jacobs et al., 1999](courtesy of Veeco Instruments Inc., Support Note 231, Revision E). GND – ground; OSC – oscillating signal applied to tip; DC – DC bias applied to tip.

Wear and triboelectric charging experiments were conducted with jumper settings as shown in Fig. 2.9.

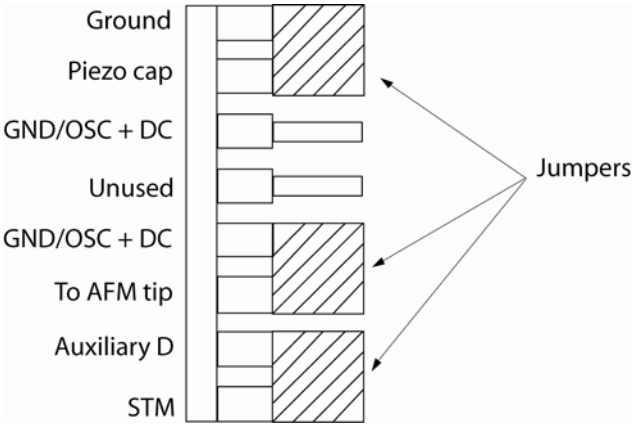

Figure 2.9 Jumper configuration during surface potential measurement for wear and triboelectric charging data.

Kelvin probe measurements are affected by a variety of parameters. Physically it is the contact potential difference between tip and sample that is being measured. This is the difference in work function between the tip and sample. Thus any change in work function will be apparent in the surface potential image as measured with Kelvin probe microscopy. Physical or chemical differences between local surface structures and temperature variations along a surface are some of the more common parameters influencing the measurement. In dielectrics, trapped charges will also play a role as will chemical or physical variations along the surface. Additionally the work function of the tip electrode is an obvious factor, as it is the difference in work function that is being measured. This explains why a measured value of 0 V is not often observed when an applied voltage is absent. A measured value near 0 V is only likely in situations where the tip and sample have similar work functions. Because potential difference is what is being measured, any of the

aforementioned parameters may also affect the tip and cause similar variations in the measured surface potential. For this reason, tips are changed regularly to avoid using tips which have been physically altered due to overuse.

Samples were mounted in conductive silver paint in most cases. In latex rubbing experiments, a piece of electrical tape was place on the sample puck, and then the sample was mounted in Liquid Paper. This was done to isolate the sample from ground to prevent discharging prior to measurement. To apply charge, an external power supply was connected to the microscope piezo cap through jumpers located in the microscope base. The jumper configuration and resulting electrical circuit schematic are shown in Fig. 2.8 as previously discussed. To produce applied potential results, the tip was engaged and an initial scan was made with 1V applied to the sample. At the completion of the scan the voltage was raised to 2V. At the completion of the 2V scan, the external power supply was turned off to collect a 0V scan. This sequence of applied voltages allowed both charging (1V-2V) as well as discharging (2V-0V) characteristics to be observed.

To check the accuracy of the technique, a sample of gold film on glass was cut with a razor blade across the top and through the gold film to the glass. This created two electrically isolated gold pads approximately 40 μm apart. Leads were connected with silver epoxy to each pad and one volt was applied across them. This is shown in Fig. 2.10. This figure shows that the topography of the gold surfaces is similar on both sides, but the surface potential is clearly one volt apart. A profile of the surface potential map is also shown for clarity (the two traces on this figure are trace and

retrace paths of a single profile). This measurement confirmed the validity and accuracy of the technique.

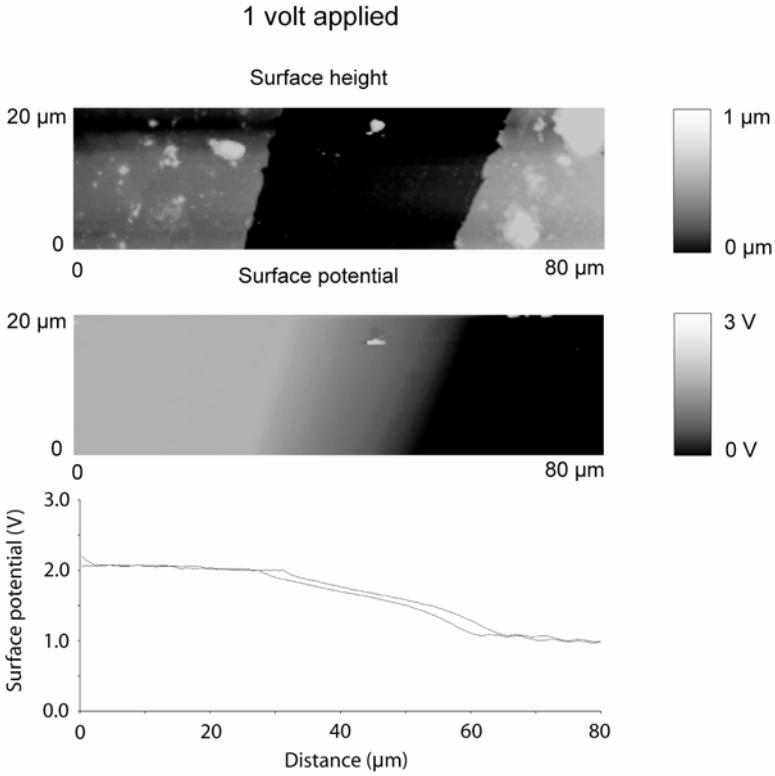

Figure 2.10 AFM images showing isolated gold pads with one volt applied across. Surface potential image and profile clearly show one volt difference is measured by Kelvin probe method.

Several scans were made on a silicon grating with trenches approximately 500 nm deep to investigate the effect of topography on surface potential measurements. 500 nm is the average height of a cuticle scale edge on a human hair. Fig. 2.11 shows a scan made perpendicular to the major height change on these features, and a scan made parallel to the major height change. It is obvious from these features that a topography effect exists, causing error in the surface potential image.

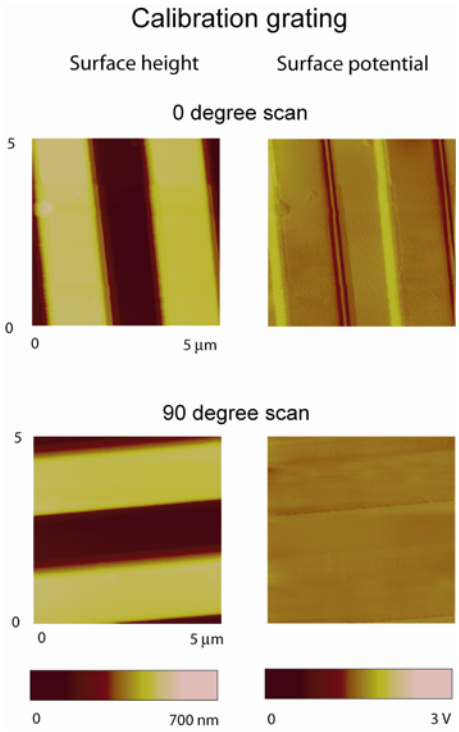

Figure 2.11 AFM images of silicon calibration grating with tip scanned perpendicular to trenches showing topography effect (trench depth is ~500 nm), and AFM images of silicon calibration grating with tip scanned parallel to trenches showing absence of topography effect.

The surface potential in the 0º scan of Fig. 2.11 is clearly more negative as the tip goes down the feature, and more positive as the tip goes up the feature, as the tip moves left to right. However, the 90º scan of Fig. 2.11 shows very little contrast in potential around the edges of the trenches. This indicates that the potential contrast seen in the 0º scan is merely an artifact caused by the topography and is not a real surface potential change. Fig. 2.12 shows a much smaller trench approximately 40 nm deep. This figure shows that smaller features do not suffer from the topography effect nearly as much.

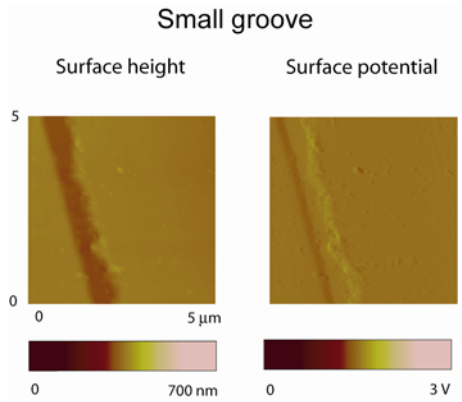

Figure 2.12 AFM images of small groove (depth ~40 nm) with tip scanned perpendicular to the groove showing less of an effect from topography.

For this reason the contrast in surface potential seen around cuticle scale edges of human hair, seen in AFM images presented later in this study, is ignored as it is likely a result of the topography effect discussed here. This effect of topography on measured surface potential is similar to an effect previously reported (Efimov and Cohen, 2000).

2.4 Samples

In this thesis, chemically damaged as well as virgin(undamaged) samples are studied. Additionally, samples both treated with PDMS (poly(dimethylsiloxane)) silicone conditioner and those left untreated are used. In some cases, virgin samples with severe cuticle damaged (mechanically damaged) and chemically damaged samples treated with amino silicone conditioner were studied. All hair samples were prepared per Appendix A. The PDMS silicone conditioner physically attaches to the hair surface, and thus remains mobile on the surface. Because of this, it constantly

redistributes and tend to coat the hair unevenly. Amino silicone conditioner is believed to chemically attach to the hair and therefore it coats evenly and remains on the hair surface without redistributing.

In surface potential studies, a variety of baseline samples were studied. Single crystal aluminum, metal particle (MP) magnetic tape, and bulk PDMS were used. The aluminum sample had a mirror polish finish and was cleaned in acetone in an ultrasonic bath for 20 min. prior to measurement. The remaining baseline samples were not treated prior to measurement. All samples were mounted in silver paint unless otherwise noted.

CHAPTER 3

RESULTS AND DISCUSSION

3.1 Contact mode and tapping mode comparison

Initial testing to compare contact mode and tapping mode was done on virgin and damaged treated (3 cycles) samples. These samples were chosen because they represent the least altered and the most altered hair samples, respectively. 5 x 5 μm images were taken at a scale edge, as well as 2 x 2 μm images away from any scale edges. Additionally, power spectrum density functions (PSDF) were plotted to show the frequencies of the captured data. These images are shown in Fig. 3.1.

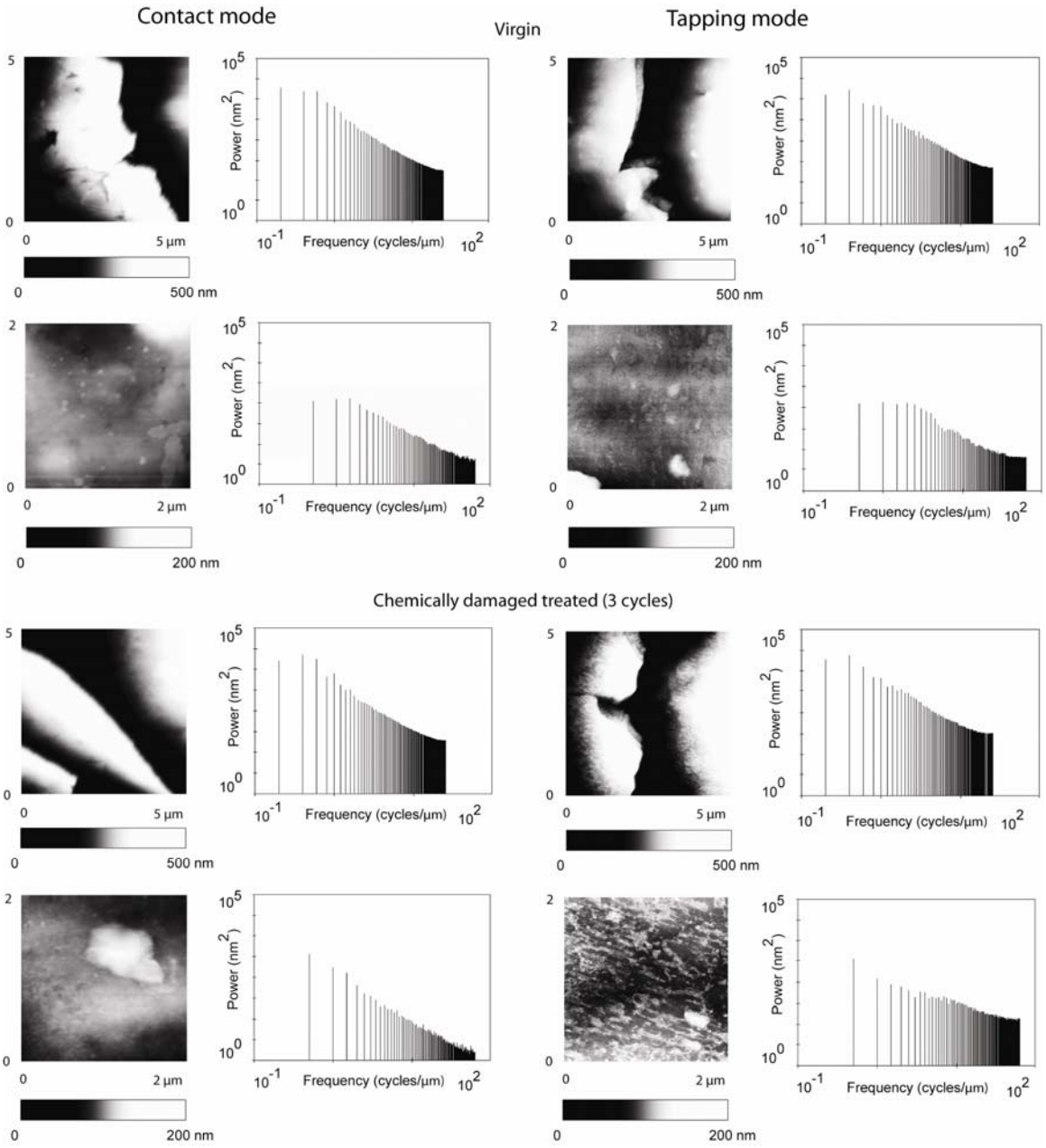

Figure 3.1 Surface height maps, and corresponding power spectrum plots for virgin and damaged treated (3 cycles) samples. 5 x 5 µm image at scale edge as well as 2 x 2 µm image away from scale edge are included. PSDFs show that tapping mode measures more high frequency data than does contact mode, especially for the treated sample.

These images show that obtaining higher resolution image was possible using tapping mode. The PSDFs also show interesting results. For the 5 x 5 µm images

there does not seem to be much difference in the frequency spectrum between contact mode and tapping mode. However, this is not the case for the 2 x 2 μm images. In the case of virgin hair, there is slightly more high frequency information present in the tapping mode image than in the contact mode image. In the damaged treated (3 cycles) sample, however, there is significantly more high frequency data being captured in tapping mode, and this is very obviously shown by the PSDF for this case. Because both image sizes use the same number of data points, the 5 x 5 μm images have significantly lower resolution that the 2 x 2 μm images, making it difficult to distinguish differences in the high frequency information, which is the goal of this study. Therefore, only 2 x 2 μm images away from the scale edge will be considered for the remaining 3 samples.

Fig. 3.2 shows surface height maps for all samples and their corresponding PSDF plots.

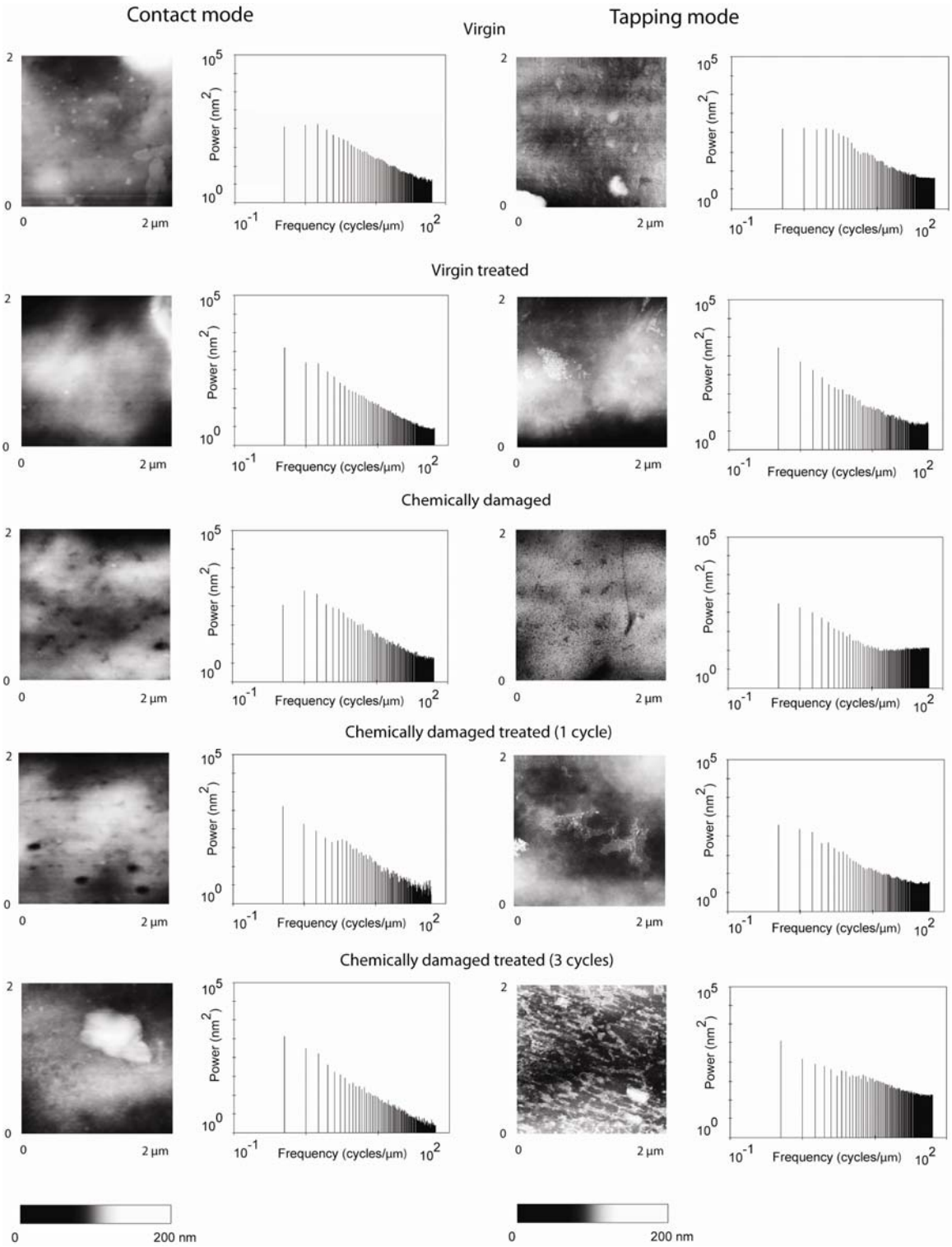

Figure 3.2 2 x 2 µm surface height images away from scale edge for all samples, measured in both contact mode and tapping mode, and their corresponding PSDFs.

Sample	Contact mode (nm^2)	Tapping mode (nm^2)
Virgin	5.8	9.3
Virgin treated	2.7	5.1
Chemically damaged	6.1	10.3
Chemically damaged treated (1 cycle)	2.5	5.3
Chemically damaged treated (3 cycles)	1.3	42.5

Table 3.1 High frequency power (> 10 cycles/um) for 2 x2 μm surface height maps away from scale edges

To compare the frequency data more easily, the power above 10 cycles/μm for each sample is tabulated in Table 3.1. Figure 3.2 and Table 3.1 clearly show that more high frequency information is captured with tapping mode than with contact mode. This is due to the fact that contact mode deforms nanoscale features on the hair surface, and thus is unable to image these small features. Tapping mode is less destructive by nature, and thus is able to capture these small features, resulting in higher frequency data. It is observed from the data that while every sample shows more high frequency data for tapping mode, this outcome is most pronounced for treated samples, especially damaged treated (3 cycles), which is believed to have the most evenly distributed conditioner layer, and thus gives the highest probability that the tip is scanning over conditioner deposits rather than the cuticle surface. This suggests that the high frequency information is an indication of conditioner on the hair surface. A reason for this is that meniscus bridges between the tip and conditioner layer may be caused creating surface features on the conditioner layer which are as small as the silicon tip itself. These tiny features could explain the high frequency data obtained. It should be noted that the differences in frequency spectra

between different samples in contact mode will not show the same relation as in tapping mode. The conclusion that high frequency data is an indication of conditioner presence is only valid with tapping mode data because contact mode will cause deformation of the small features leading to the high frequency data. Therefore, as is observed, treated samples will appear smoother (less high frequency data) than untreated samples in contact mode, but will exhibit more high frequency data than untreated samples in tapping mode. Similarly, features are observed visually on the treated samples imaged in tapping mode that are absent on the untreated samples, and are never seen in contact mode images. Again this suggests that what is being observed are actual conditioner deposits. It is then concluded that because of its non-destructive nature, tapping mode is able to image actual conditioner deposits, making it possible to visually observe where conditioner remains on the hair surface. This is in contrast to contact mode, where conditioner deposits are never seen visually in the surface height maps. This is due to the fact that contact mode allows for localized plowing of the soft conditioner deposits. Conditioner deposits are therefore not captured in the surface height maps using contact mode.

Previous studies have suggested that the majority of conditioner remains near the scale edge bases after application[8]. These claims have been made based on friction and adhesion data showing higher friction and adhesion at the scale edge bases. Due to the fact that tapping mode is able to image conditioner deposits, whereas contact mode is not, images were taken at the scale edge bases at a high magnification (2 x 2 μm) in tapping mode, as shown in Figure 3.3.

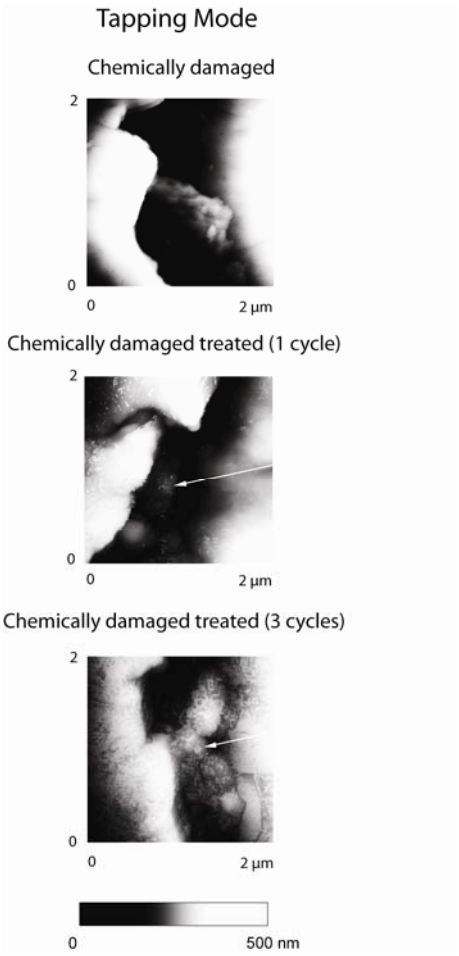

Figure 3.3 Tapping mode surface height images of 2 x 2 µm size at scale edge. Arrows indicate locations of visible conditioner deposits.

The features previously found on treated samples, and determined to be conditioner deposits, are seen in large amounts near the scale edge bases of these images. These areas are shown with arrows in the figure. The damaged treated (3 cycles) sample shows a higher presence of conditioner than does the damaged treated (1 cycle) sample. This is expected as it is believed that the sample treated with 3 cycles of conditioner maintains a thicker conditioner film than does the sample treated with only 1 cycle.

While tapping mode gives an indication of conditioner on the hair surface, Si is hydrophilic, and therefore may pick up and transfer conditioner as it scans the surface. For this reason it should be understood that conditioner deposits as they appear in the surface height maps have likely been altered or moved on the hair surface by the tip itself. However because tapping mode does not alter the conditioner deposits by plowing in the lateral direction, it is still capable of imaging conditioner deposits whereas contact mode is not.

3.2 Conditioner thickness and adhesive force mapping

To help further understand where conditioner deposits on hair surface, mapping conditioner thickness is performed. Figure 3.4(a) shows typical force calibration plots (extend direction only) for damaged, damaged treated (1 cycle), and damaged treated (3 cycles) samples. These plots demonstrate the effect a conditioner film has on the tip/sample interaction. Figure 3.4(b) shows force calibration plots for a damaged treated (3 cycles) sample both at the scale edge base, and away from the scale edge.

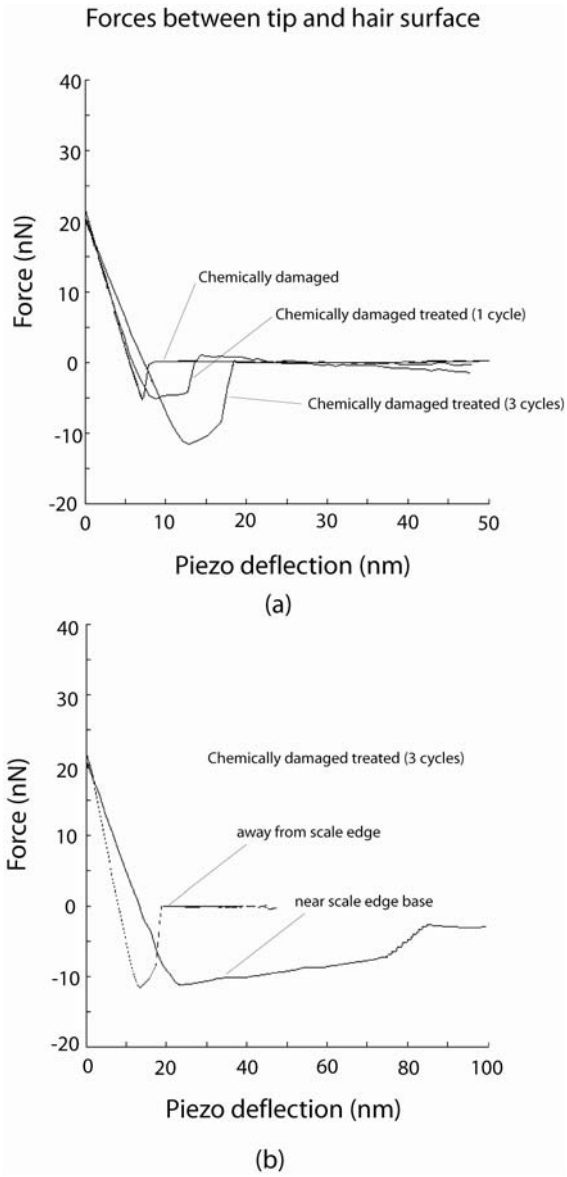

Figure 3.4 (a) Typical force calibration plot (extend portion only) showing the difference between damaged samples with varying levels of conditioner treatment. ; (b) Typical force calibration plot (extend portion only) showing the difference for damaged treated (3 cycles) at the scale edge base and away from the scale edge. The attractive forces are believed to be unaffected by the thickness of the conditioner layer, and the tip easily passes through the conditioner, lending to the similar values of force for both samples.

It is evident from this figure that the conditioner thickness is much higher at the scale edge base than it is on the surface away from the scale edge. This supports

previous claims that the majority of conditioner remains at the scale edge base, as discussed earlier. Similar plots were taken as discrete points, per the explanation in section 2.1 of this thesis, to create thickness and adhesion maps, which are shown in Figure 3.5.

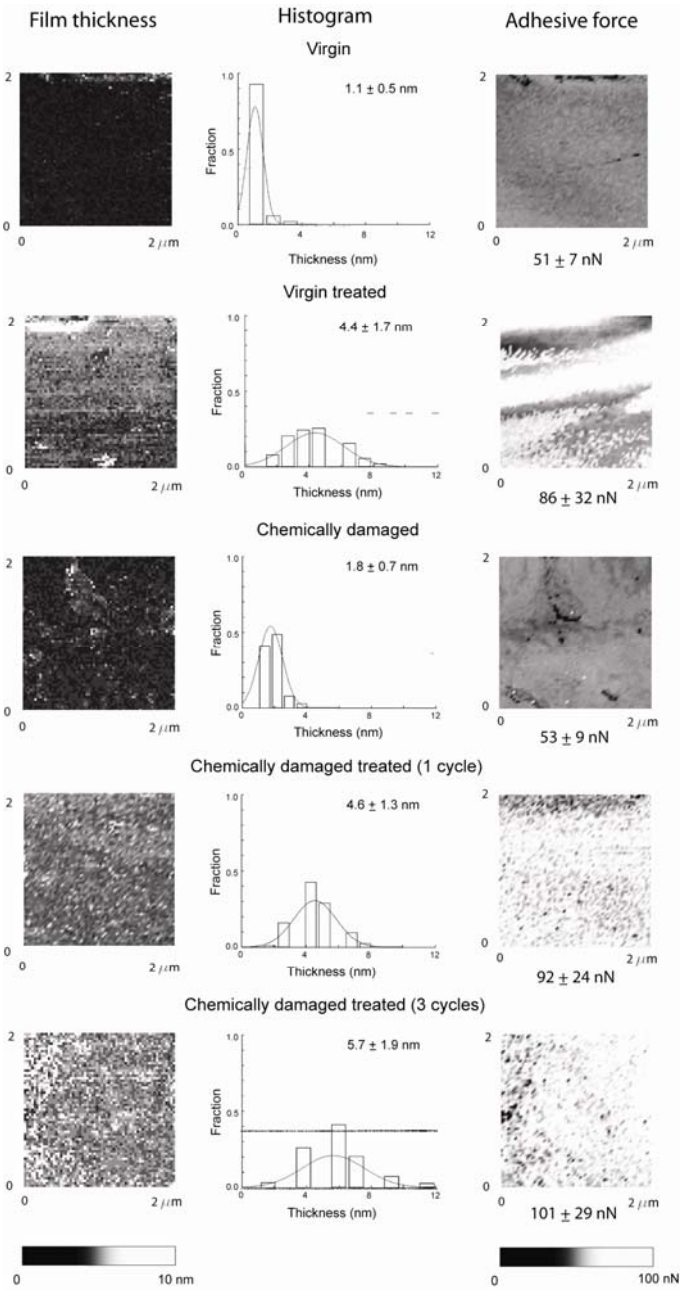

Figure 3.5 Film thickness and adhesive force maps for all samples. Maps are for areas of 2 x 2 μm size, away from scale edges. Histograms of thickness distribution are also shown.

Virgin hair shows a mean thickness of 1.1 nm, with a very narrow distribution. The outermost layer of virgin hair surface is made up of fatty acid, as previously discussed[2, 3, 5], which makes the hair surface hydrophobic (contact angle is about 103°)[5]. Due to its hydrophobicity, virgin hair surface is absent of any water film, and therefore film thickness on the surface is measured as very low. Damaged hair, however, is slightly hydrophilic due to the removal of the fatty acid layer during damaging process (contact angle 50-80°)[5]. Therefore, a continuous water film may be present, which explains the slightly higher mean film thickness of 1.8 nm and slightly wider distribution. The results of virgin and damaged samples show a finite thickness will be measured even in the absence of conditioner for the reasons stated above. However, as previously discussed, it is known that this technique overestimates the film thickness. Based on the results from virgin and damaged samples this overestimation is determined to be 1-2 nm. Virgin treated and damaged treated (1 cycle) samples are comparable and are measured to have 4.4 nm and 4.6 nm mean film thickness, respectively. Additionally, they have distributions 2-3 times wider than the untreated samples. As was previously suspected damaged treated (3 cycles) sample has the highest mean thickness at 5.7 nm with a distribution slightly higher than the other treated samples. Local maxima on the general hair surface away from cuticle edges on all treated samples were observed to reach as high as 25 nm (data not shown). The distribution of thickness widens with increased conditioner cycles because the conditioner is believed to distribute unevenly on the hair surface. Therefore as more conditioner is deposited on the hair surface, the range of thicknesses grows. The adhesive maps show similar trends with untreated samples

having low adhesion, and treated samples having higher and increasing with additional conditioner applications. As the amount of conditioner on the hair surface increases, the possibility of creating a meniscus bridge between tip and sample increases. When such a meniscus bridge is created, the meniscus force (given by Eq. 2.1) will dominate the adhesion. This adhesive mechanism explains the trend of higher adhesive force with more conditioner application. This data is also shown in Table 3.2.

Sample	Conditioner Thickness (nm)	Adhesive Force (nN)
Virgin	1.1 ± .5	51 ± 7
Virgin treated	4.4 ± 1.7	86 ± 32
Chemically damaged	1.8 ± .7	53 ± 9
Chemically damaged treated (1 cycle)	4.6 ± 1.3	92 ± 24
Chemically damaged treated (3 cycles)	5.7 ± 1.9	101 ± 29

Table 3.2 Mean conditioner thickness and adhesive force values

As previously stated, the majority of conditioner is thought to remain near the scale edge bases on the hair surface. To verify this, thickness maps were created at scale edges, as is shown in Figure 3.6.

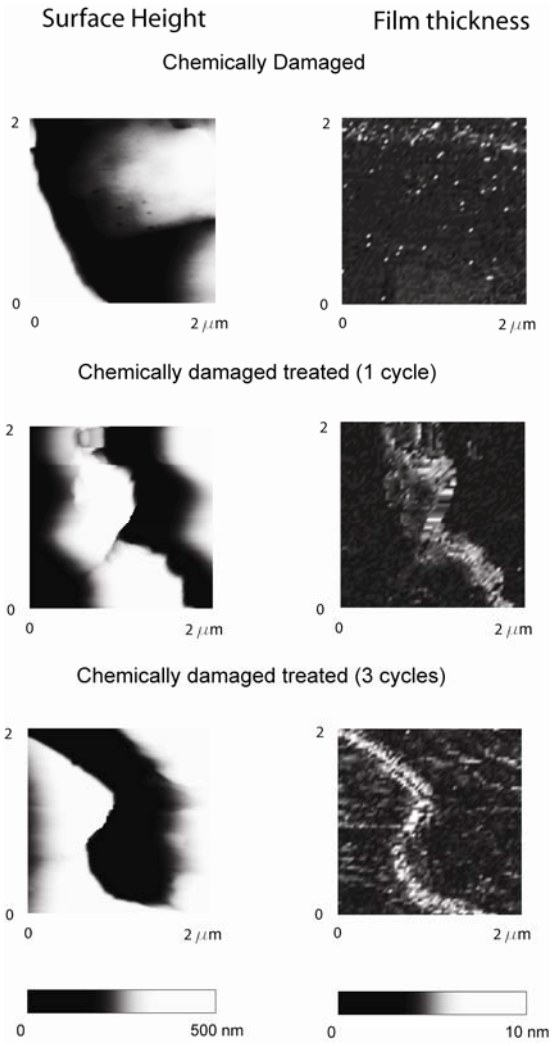

Figure 3.6 Surface height maps and corresponding film thickness maps for damaged samples of varying conditioner treatment. Thickness maps clearly show that conditioner deposits heavily at scale edge base.

Damaged sample is shown as a baseline, demonstrating that the increase in measured thickness at the scale edge base is a real increase in conditioner thickness, and not an effect of the scale edge itself. The thickness maps of damaged treated (1 cycle) and damaged treated (3 cycles) clearly show a higher film thickness at the edge

of the scale, which is shown by comparing the thickness maps to their corresponding height maps. Conditioner thickness at the scale edge base was found to be 30-100 nm in depth (data not shown).

As previously stated, conditioner may be picked up by the hydrophilic Si tip, and consequently transferred on the surface. However, it is assumed that the amount of conditioner picked up by the tip is small, and remains relatively constant throughout the measurements. This being the case, the slight overestimation in film thickness due to conditioner remaining on the tip will remain constant, and the difference between thickness at the scale edge and that away from the edge remains accurate.

3.3 Friction and adhesion measured with hydrophobic tip

Because the interaction of hair with finger skin is extremely common in the real world, measuring friction and adhesion by simulating this interaction is of interest. As previously discussed, uncleaned finger skin tends to be hydrophilic while cleaned finger skin tends to be hydrophobic. For this reason it is of interest to measure tribological properties with a hydrophobic tip, in addition to the previous work with hydrophilic tips. Fig. 3.7 shows the adhesive force maps made with the coated tip and with an uncoated tip, and the corresponding average adhesive force values. The adhesive force data is summarized in Table 3.3 and also in Fig. 3.8(a). Figure 3.8(b) presents a summary of coefficient of friction data measured both with an uncoated and a coated tip.

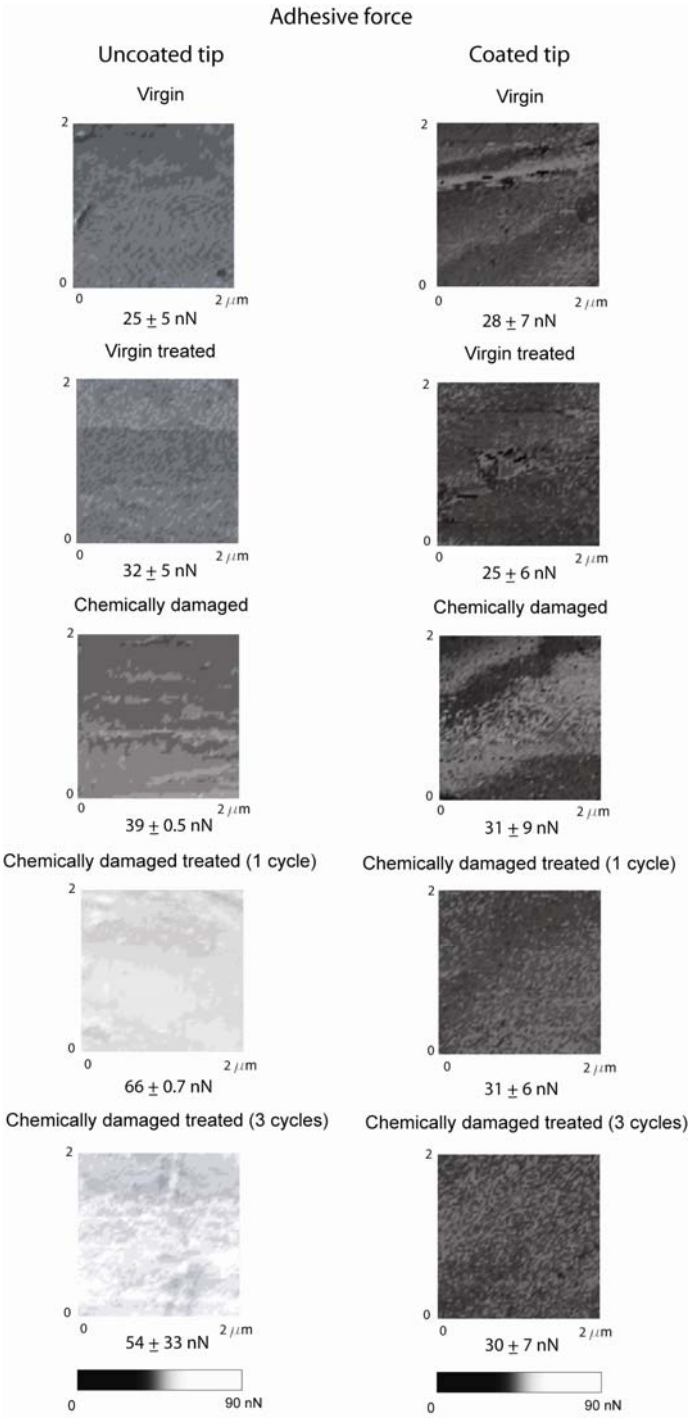

Figure 3.7 Adhesive force maps over 2 x 2 μm area away from scale edges taken with coated, hydrophobic Si_3N_4 tip as well as uncoated Si_3N_4 tip.

	Coefficient of friction		Adhesion	
Sample	Uncoated	Coated	Uncoated	Coated
Virgin	.03 ± .001	.03 ± .006	25 ± 5	28 ± 7
Virgin treated	.03 ± .009	.02 ± .004	32 ± 5	25 ± 6
Chemically damaged	.22 ± .03	.05 + .004	39 ± .5	31 ± 9
Chemically damaged treated (1 cycle)	.05 ± .01	.02 ± .001	66 ± .7	31 ± 6
Chemically damaged treated (3 cycles)	.05 ± .02	.03 ± .006	54 ± 33	30 ± 7

Table 3.3 Coefficient of friction and adhesion measured with both coated and uncoated tips

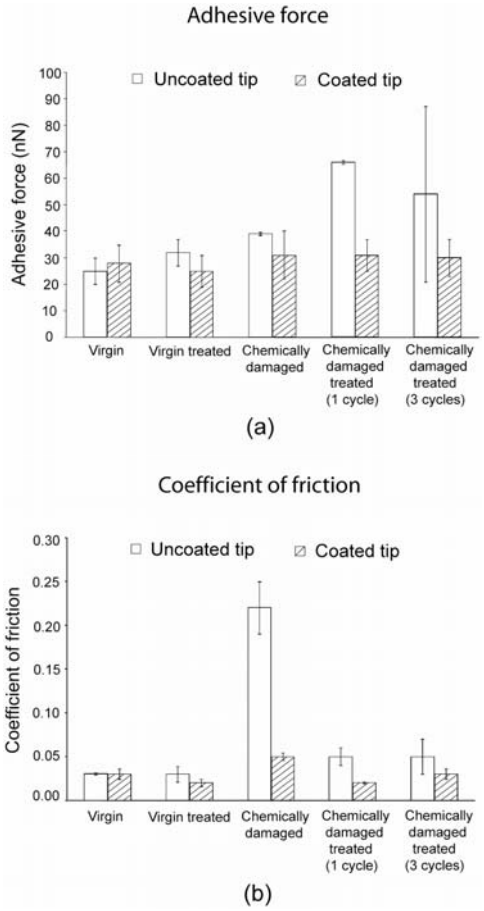

Figure 3.8 (a) Comparison of coefficient of friction taken with both coated and uncoated tips ; (b) Comparison of adhesive force taken with both coated and uncoated tips. Uncoated tip adhesive force data is taken from LaTorre and Bhushan (2005b).

The data in Fig. 3.8 shows that there is no obvious trend in friction or adhesion as a function of conditioner application when measured with a coated tip. This is in strong contrast to the values measured with the uncoated tip. For uncoated tip measurements, friction tends to decrease with conditioner application, and adhesive force tends to increase.

In general there is only a slight decrease in friction, for all but the chemically damaged sample, between values measured with a coated tip and those measured with an uncoated tip. This trend, shown in Fig. 3.8(b), can be attributed to the lubricating properties of Z-TETRAOL and the variability of human hair. However, the difference in coefficient of friction values for damaged hair is clearly a result of meniscus forces being absent in the coated tip scenario. Because chemically damaged hair is hydrophilic[11], when measured with a hydrophilic tip meniscus forces strongly contribute to the friction. When measured with a hydrophobic tip, however, this large increase in friction force in damaged hair is not observed. This clearly shows the large effect meniscus forces play in the trends observed in friction on the nanoscale. It should be noted that the same trend is not observed in virgin hair because virgin hair is slightly hydrophobic, so meniscus forces will not be nearly as significant, regardless of tip contact angle.

Adhesive force results shown in Fig. 3.7 and Fig. 3.8(a) indicate the same mechanisms determined from coefficient of friction results. Again, virgin hair is hydrophobic, so the contact angle of the tip will not have a significant effect on the results. However, it is observed that for a hydrophilic uncoated tip, adhesive force increases significantly with conditioner application for damaged samples. This is not

the case when measured with a coated tip, as adhesive forces remain relatively constant for all samples when measured with the coated tip. This again suggests that meniscus forces contribute significantly to adhesion on the nanoscale. With the addition of conditioner to the damaged hair surface, meniscus bridges between the hydrophilic tip and conditioner will form, greatly increasing the force required to pull the tip from the surface. When a hydrophobic tip is used, this is not observed, as is expected.

3.4 Dynamic contact angle

3.4.1 Directionality dependence

There are two significant directionality effects using the Wilhelmy balance technique. The first is the contrast between forces measured in the advancing direction and those measured in the receding direction. This issue has been discussed in section 2.2, and will not be discussed further here. The other involves the orientation of the hair fiber in the measurement setup. Caucasian virgin samples were measured in both fiber orientations and compared, as shown in Fig. 3.9.

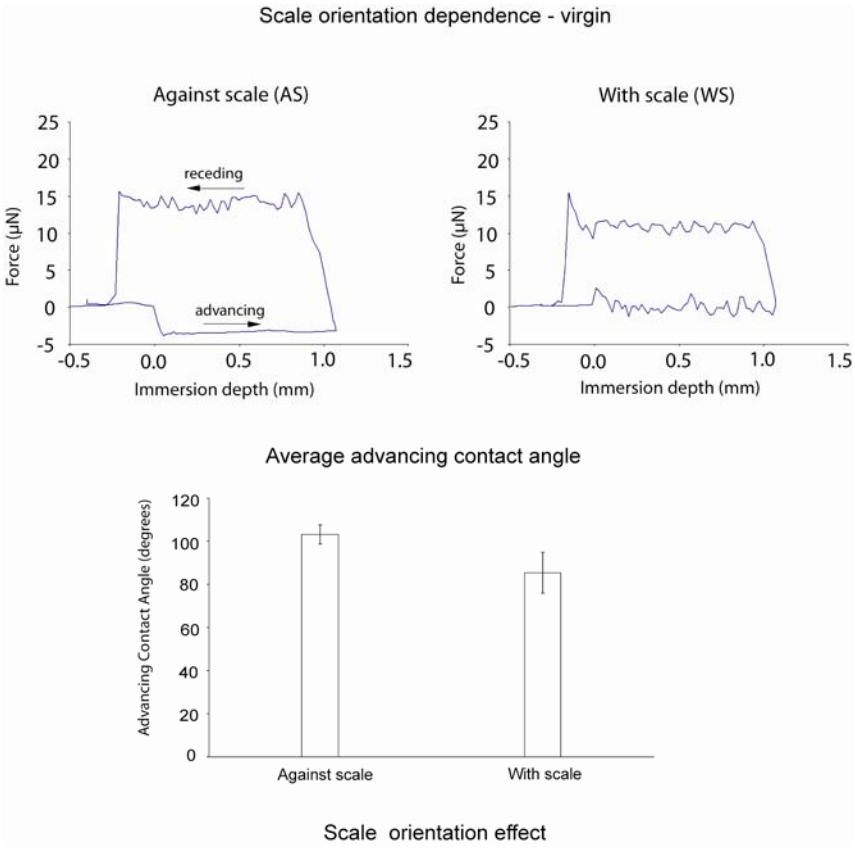

Figure 3.9 Force curves and average advancing contact angle values for virgin hair in both against scale (AS) and with scale (WS) orientations. Contact angle value is observed to be lower for the WS direction.

It is evident here that fibers oriented in the with scale (WS) orientation exhibit lower advancing contact angles than those in the against scale (AS) orientation. The reason for this is shown in Figure 3.10. Here it is shown that for the advancing direction, the AS orientation creates a situation in which the liquid does not come in contact with the scale edges at the liquid/air interface. However, for the WS orientation, the scale edges are fully wetted at the liquid/air interface as the hair pushes through the liquid surface. Being that the scale edges are far more prone to

mechanical damage than the cuticle surface away from the edges, and all hair samples will exhibit some degree of mechanical damage which is unavoidable due to handling, the scale edges tend to be more hydrophilic than the rest of the hair surface.

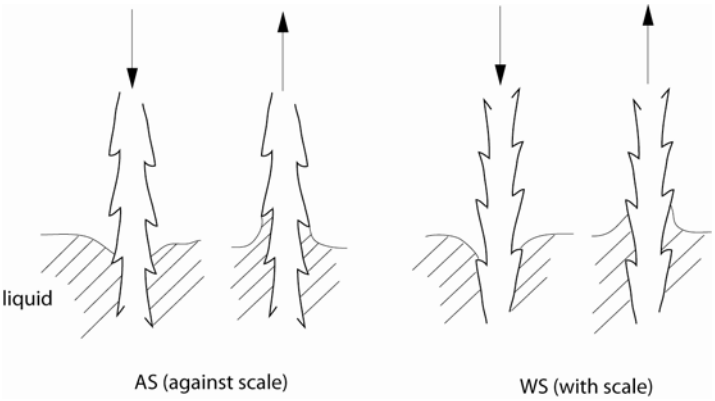

Figure 3.10 Schematic showing mechanism for result shown in Fig. 3.9. WS advancing direction correlates to contact angle values heavily influenced by scale edge contributions.

This being the case, the WS orientation exhibits a lower contact angle than the AS orientation because the scale edges are more easily wetted in the WS orientation. This result is in contrast to that reported by Molina where it was determined there was no effect of scale orientation on advancing contact angle. Molina did report, however, that the receding mode was affected in the same manner that was found in the present study. However, the data presented in Fig. 3.9 shows an obvious advancing mode force dependence on scale orientation, and the argument given here and shown in Fig. 3.10 explains this dependence. It is possible the hair fibers used in this study exhibited thicker cuticle scales for any variety of reasons, which would make the effect more noticeable. Thinner cuticle scales would cause less of an effect, perhaps

making it unnoticeable, indicating no difference as reported by Molina. Because the AS orientation relates to wetting properties of the scale surface instead of the scale edge, all further data is given for fibers in the AS orientation.

3.4.2 Conditioner treated hairs and environmental effect

The five samples of interest in this section are Caucasian virgin, virgin treated, chemically damaged, chemically damaged treated (1 cycle), and chemically damaged treated (3 cycles). Five samples were measured for each type of hair. The force plots are shown in Figure 3.11. Average advancing contact angle values are shown in Fig. 3.12 and Table 3.4.

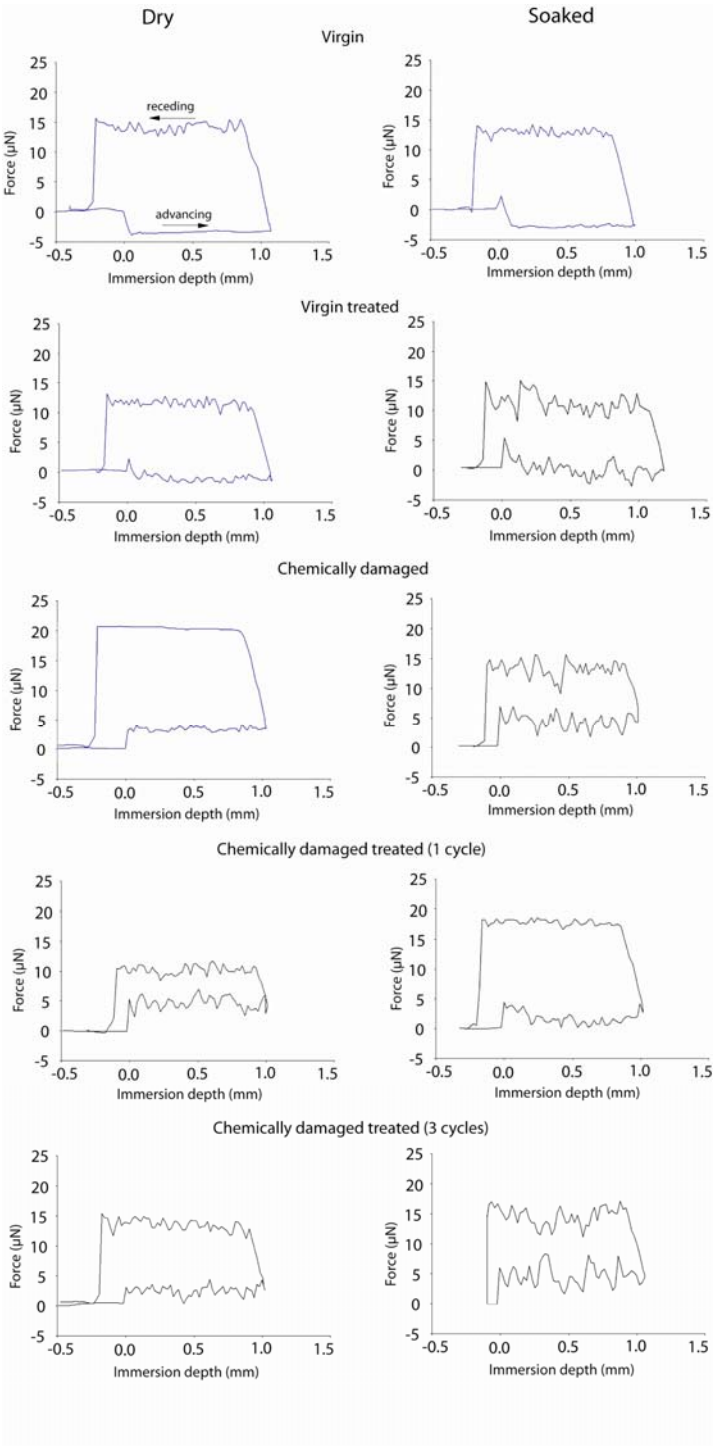

Figure 3.11 Force curves for five Caucasian samples for both dry and wet scenarios.

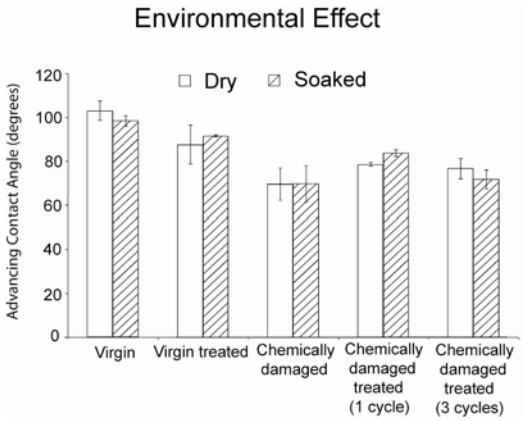

Figure 3.12 Average advancing contact angle values for five Caucasian samples for both dry and wet conditions.

Sample	Contact angle (deg.)	
	Dry	Soaked
Virgin	103 ± 4	98 ± 2
Virgin treated	88± 9	92± 1
Chemically damaged	70 ± 7	70 ± 8
Chemically damaged treated (1 cycle)	79 ± 1	84± 2
Chemically damaged treated (3 cycles)	77 ± 5	72 ± 4
Asian	95 ± 4	--
African	92 ± 11	--
Mechanically damaged	80 ± 14	--
Virgin – with scale (WS) orientation	85 ± 10	--

Table 3.4 Summary of average advancing contact angle values

Virgin hair was measured first, and a value of 103º was obtained. This agrees well with values measured by Molina *et al*. It was found that chemically damaged hairs exhibit a much lower contact angle than do virgin hairs. In this study p values were used to determine if the variations in contact angle value for different samples were statistically significant. A p value is the probability that significance is found where there really is none (p=.05, 5% chance significance is declared where it does not exist). A p value of 0.00005 was found for the difference between virgin and chemically damaged hairs. This is strong evidence that the difference is real, as it

indicates only a 0.005% chance that the difference is not real. This trend is also the same as in previous studies[16,17]. The reason for this, as mentioned earlier, is that the hydrophobic outermost layer of virgin hair, the cell membrane complex, is partially removed during damage, exposing hydrophilic underlayers. A schematic of this surface structure is shown in Fig. 1.1. Additionally, conditioner treatment was found to lower the contact angle of virgin hair (p value of 0.0075) and increase the contact angle of chemically damaged hair (p value for chemically damaged and chemically damaged treated (1 cycle) is 0.024). These results explain previous findings that virgin hair exhibits a lower coefficient of friction than chemically damaged hair[8,16,17]. The p value for the difference between chemically damaged treated (1 cycle) and chemically damaged treated (3 cycles) was found to be 0.36. This indicates multiple conditioner applications may not affect the wetting properties of the hair. Because the damaged surface is hydrophilic, meniscus forces may contribute a significant portion to the total friction force, whereas this is not the case for the hydrophobic virgin hair surface. For the case of conditioner treated samples two things are altered: contact angle of the surface and shearing force required. For virgin hair, treatment reduces the contact angle slightly, but it tends to remain very near 90º, so meniscus forces will not likely be significant. Also, because the virgin hair surface is already rather lubricious due to the lipid layer that is present, the addition of conditioner does not significantly add to the lubricity of the surface on the nanoscale. For these reasons, the coefficient of friction does not change much in virgin hair with conditioner treatment[8,16,17]. This, however, is not the case for chemically damaged hair. Addition of conditioner to chemically damaged hair raises the contact angle, so

less meniscus forces are present. It also creates a lubricious layer that does not exist on damaged hair, since the natural lipid layer has been removed due to the damage. The combination of these effects significantly decreases the coefficient of friction[8,16,17].

It is observed that conditioner treatment has opposite effects on virgin and damaged hairs. One explanation for this is that on virgin hair, a low energy surface is intact due to the lipid layer present. Therefore when the conditioner deposits the cationic surfactants will orient such that the alkyl chains are toward the hair surface and the cationic groups are out. The higher energy cationic groups cause a decrease in contact angle. However, for chemically damaged hair, the cationic groups will tend to orient toward the hair, leaving the alkyl chains away from hair surface, causing a decrease in surface energy and an increase in contact angle. However, the chemical interactions just proposed cannot be proven without separating each component and testing them individually, which is difficult. Another possible explanation for the effect of conditioner treatment is that if the conditioner material dominates the wetting properties of the fiber, treatment will not necessarily increase or decrease the surface contact angle, but rather cause a convergence to an angle representative of the conditioner used in the treatment. Therefore, it may be that the contact angle of the conditioner material coincidentally lies between that of virgin and damaged hair, and with treatment contact angles converge to this value. In order to further understand this converging behavior, chemically damaged hair that was treated with a conditioner containing an amino silicone was also measured. Amino silicone conditioner is known to bind to the hair surface and does not redistribute[17].

This is in contrast to commercial conditioner which is mobile on the hair surface. Therefore, amino silicone treated hair will be less affected by immersion in the wetting liquid. The contact angle of the amino silicone treated hair was found to be 75º $\pm$ 1º, which is similar to chemically damaged hair treated with commercial conditioner. This suggests that the contact angle of treated hair is indeed representative of the wetting properties of the conditioner itself.

Additionally, the force plots shown in Figure 3.11 for the dry samples indicate the probable location of conditioner deposits. As previously discussed, the receding portion of the force plot is strongly influenced by scale edge contributions, which likely have significant hydrophilic regions. This affects the force plots by giving a large hysteresis. If the scale edges are covered or hidden from proper wetting, however, this hysteresis should be smaller as the hydrophilic edges then contribute less to the receding force. It can be observed from Figure 3.11 that the untreated samples have significantly greater hysteresis than do the treated samples. This is an indication that the conditioner remains at the scale edge bases, hiding the edges from proper wetting. This agrees well with previous claims[8].

These hair samples were also soaked in deionized water for 5 minutes, and then measured to determine the effect of a wet environment on contact angle. This data is also shown in Fig. 3.11. The figure shows that the contact angle values after the samples had been soaked are nearly identical to those that were measured on dry samples. This suggests that even when subjected to a liquid water environment, the wetting properties of hair do not change with time. That is, after having been exposed to liquid water, the water still wets the surface with the same contact angle

that it did before the hair was exposed to liquid water. This also shows that soaking for 5 minutes does not remove a significant amount of the conditioner layer on treated hairs, as the contact angle does not return to the untreated value after having been soaked. It should be noted that single hair fibers exhibit a high rate of drying and thus may be changing during the experiment.

3.4.3 Damage dependence

In addition to chemical damage, samples affected with mechanical damage were also studied to compare the effects of various types of damaging treatments. These mechanically damaged samples were not damaged in a controlled way, but were observed under a 100x optical microscope to exhibit severe cuticle damage. The results of this experiment are shown in Fig. 3.13.

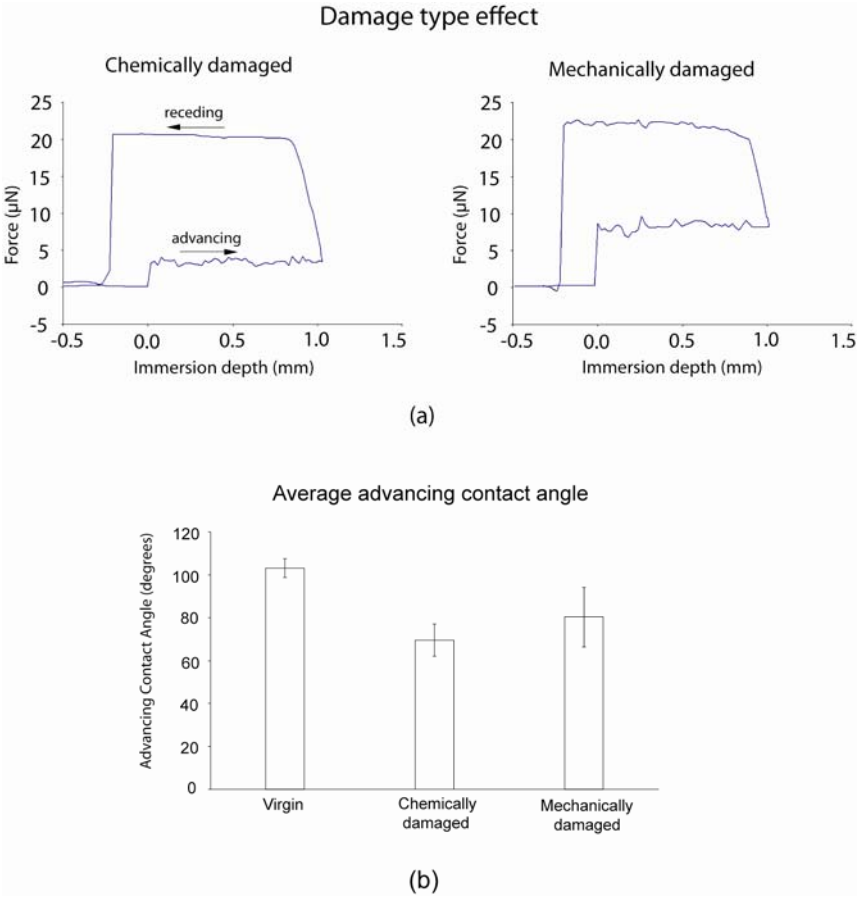

Figure 3.13 (a) Force curves comparing chemical and mechanical damage effects ; (b) Average advancing contact angle comparing chemical and mechanical damage effects.

These results show that chemically damaged hair tends to be more hydrophilic than mechanically damaged hair. However, the mechanical damage occurs primarily at the scale edges. Due to the orientation of the hair fiber (AS), the contributions to the contact angle measurement from surface material around the scale edges is very low due to the way the fiber interacts with the wetting liquid as it pushes into the liquid (shown in Fig. 3.9 and discussed earlier). Due to the geometry of the hair fiber, the majority of the contact at the liquid/air interface is on the general surface of a cuticle scale, away from scale edges. Therefore, even though the mechanical damage

exposes hydrophilic underlayers, this effect is only observed when the damage extends well beyond the scale edge. In contrast, the chemical damage occurs over every part of the hair surface, so its effect is more pronounced using this measurement technique. A method to mechanically damage the hair surface away from the scale edges, or a different measurement technique, would have to be used to more appropriately compare damaging treatments.

3.4.4 Ethnicity dependence

Virgin samples of Caucasian, African, and Asian hair were measured and compared. Results are shown in Fig. 3.14. No significant difference was found, although African and Asian hairs do exhibit a slightly lower contact angle that Caucasian hair on average. Further study would have to be done to investigate whether this difference was real or simply a result of the low number of samples measured.

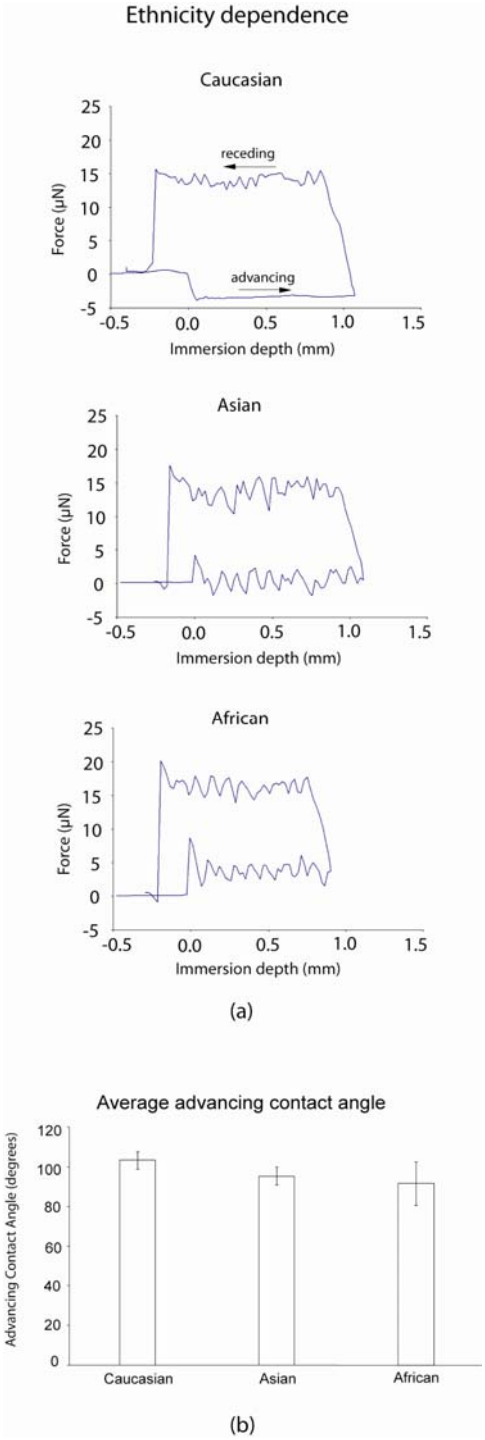

Figure 3.14 (a) Force curves showing ethnicity dependence ; (b) Average advancing contact angle values showing ethnicity dependence. No significant dependence on ethnicity was found for advancing contact angle values.

3.5 Surface potential

3.5.1 Applied potential

3.5.1.1 Baseline materials

The AFM images in this portion of this thesis are presented in three columns. The first is the surface height of the sample and the second is the absolute surface potential. The final column shows the same surface potential data as the second column, but the average surface potential (which is presented in the subsequent bar charts) is subtracted out and the scale is reduced to show more contrast. Fig. 3.15 shows the AFM images for aluminum, MP tape, and PDMS.

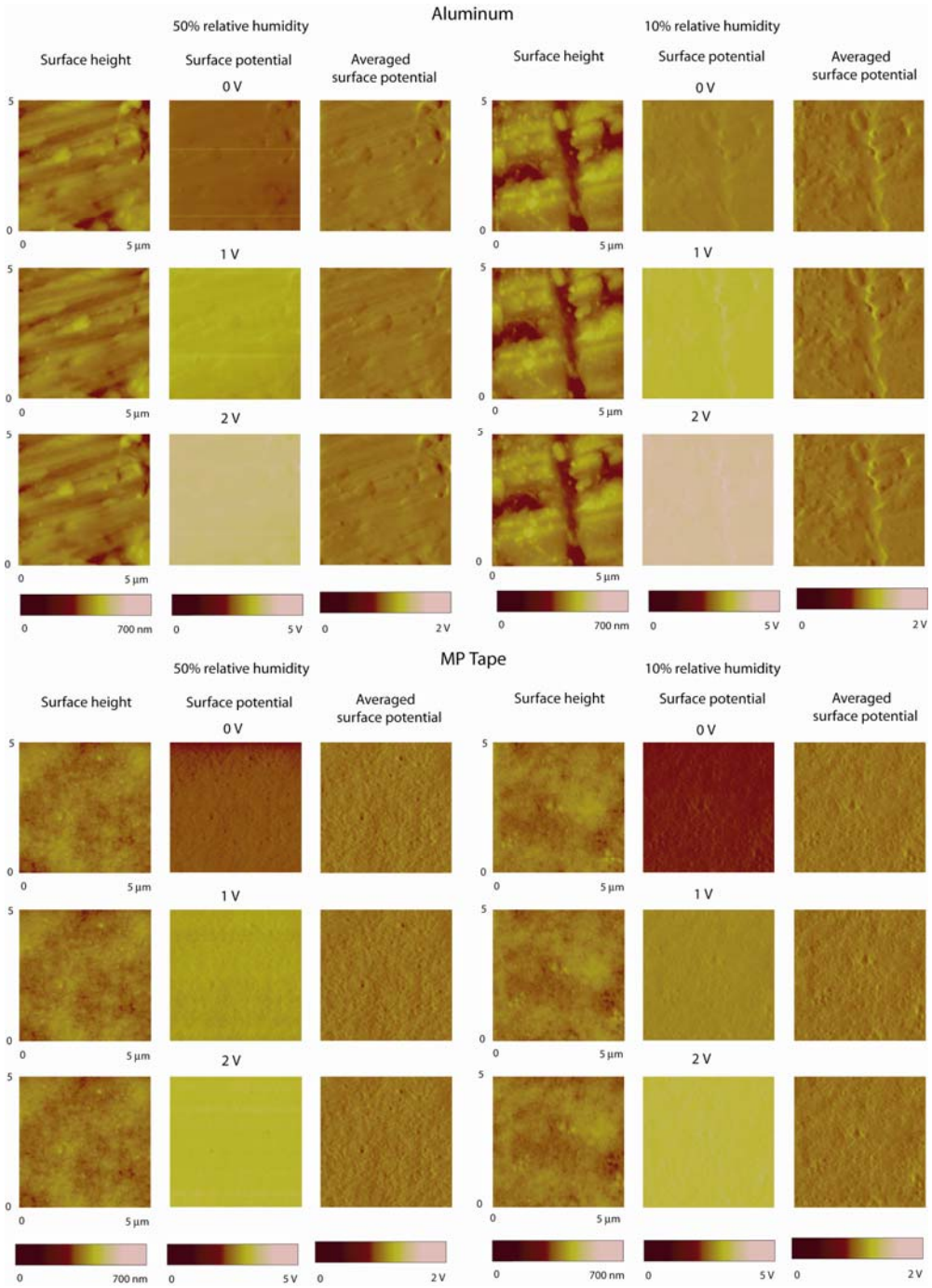

Figure 3.15 AFM images of Aluminum, MP Tape, and PDMS. (continued on next page)

Figure 3.15 (continued)

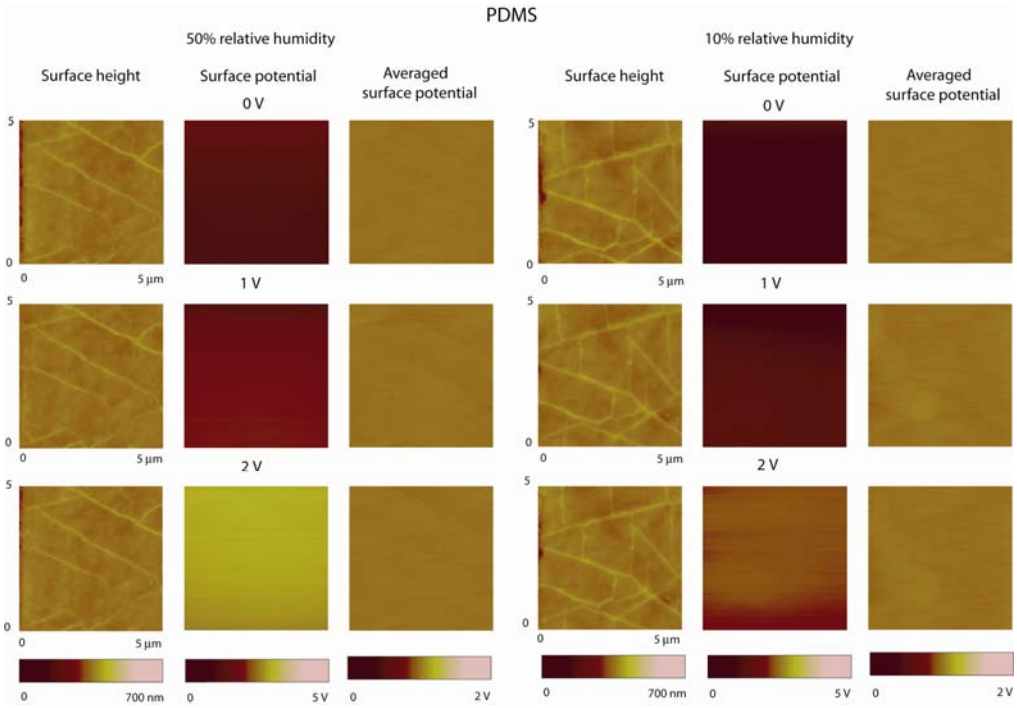

Fig. 3.16 shows the average surface potential for each sample, as well as the average surface potential change in both environments. Error bars represent +/- one standard deviation. Please note that these bar charts are on a different scale than the bar charts for hair samples. From Fig. 3.16 it is evident that the humidity does not affect the surface potential of aluminum much, MP tape to a small extent, and noticeably in PDMS. It is believed that this occurs because water vapor in the air is a significant contributor to conductivity and surface charge mobility in materials that are not very conductive. This reasoning explains the trend seen here. From this data

we understand the desire to increase conductivity in hair samples. With increased conductivity, a reduced relative humidity does not affect the surface charge nearly as much as with lower conductivity.

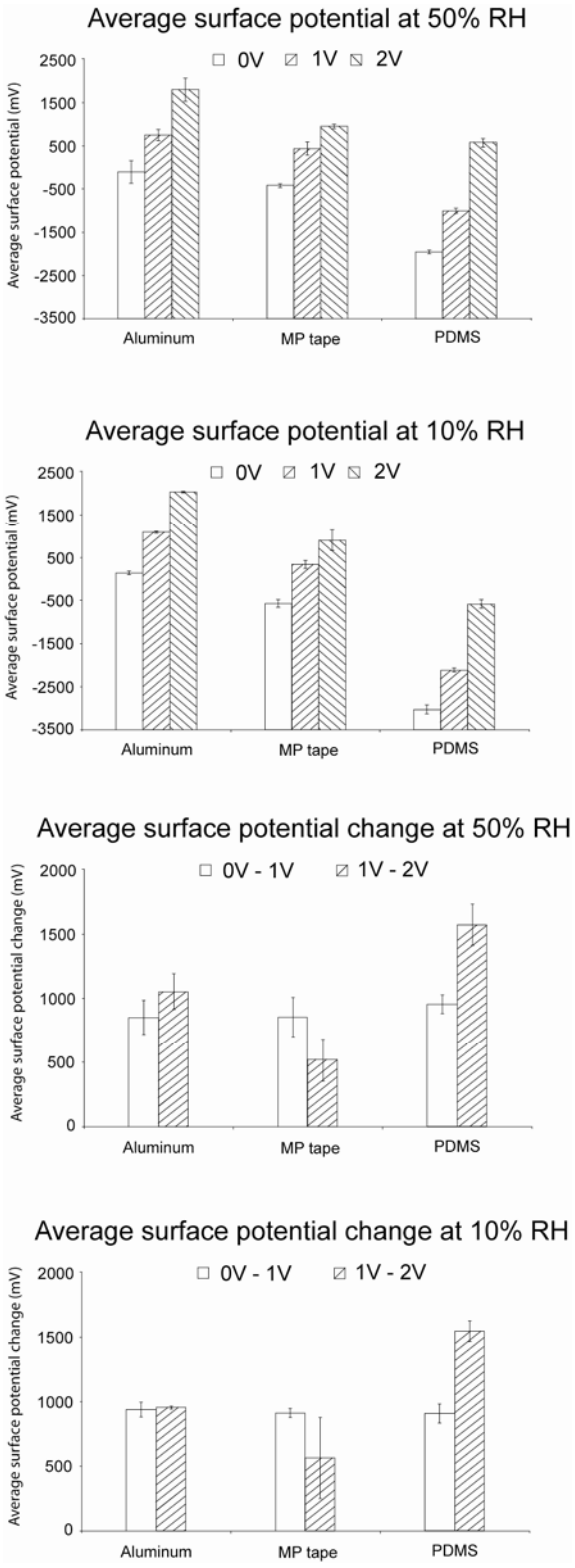

Figure 3.16 Bar charts showing average surface potential at both 50% and 10% relative humidity.

3.5.1.2 Conditioner treated hair samples

Fig. 3.17 shows AFM images for virgin, virgin treated, chemically damaged, chemically damaged treated (1 cycle), and chemically damaged treated (3 cycles). Again, it should be noted that the contrast seen around cuticle scale edges is likely a result of the topography effect described earlier, and will not be discussed further here. A key point shown by these images is the existence of areas of trapped charge in the low humidity samples. This is not seen in the samples measured in ambient. These areas of trapped charged are seen as bright areas on the sample, not corresponding to a change in topography. This indicates that water vapor in the air contributes significantly to the mobility of surface charges on the hair. This result has been previously reported for macro studies on surface charge of hair (Jachowicz *et al.*, 1985; Lunn and Evans, 1977; Mills *et al.*, 1956). Trapped charges are most pronounced in the untreated samples. This suggests that conditioner treatment has a similar effect as water vapor. Even under very low humidity conditions, conditioner treatment increases the mobility of surface charges, dissipating trapped charges. Fig. 3.18 shows bar charts of the average surface potential. Error bars indicate +/- one standard deviation. It can be observed in these figures that all samples exhibit very similar values in the 50% relative humidity scenario. This again indicates that the water vapor in the air plays a significant role on the surface charge of the hair, and also on the mobility of charge. The charts showing potential change reflect this

behavior as well. For the 50% case it is shown that the potential changes nearly 1V for every 1V change in applied potential. However, this is not the case for the 10% relative humidity situation.

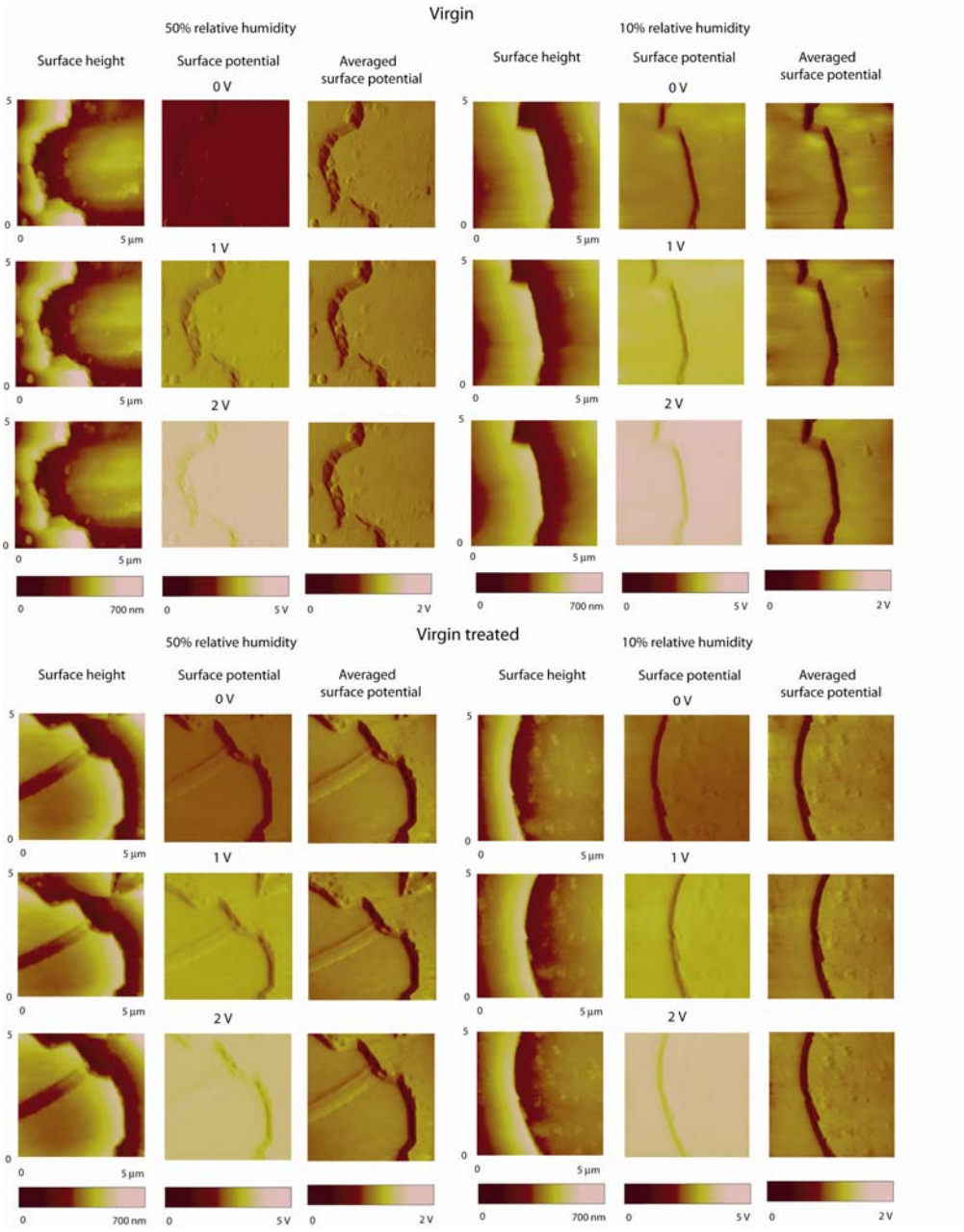

Figure 3.17 AFM images showing surface height and surface potential of virgin, virgin treated, chemically damaged, chemically damaged treated (1 cycle), and chemically damaged treated (3 cycles) hair samples. (continued on next page)

Figure 3.17 (continued)

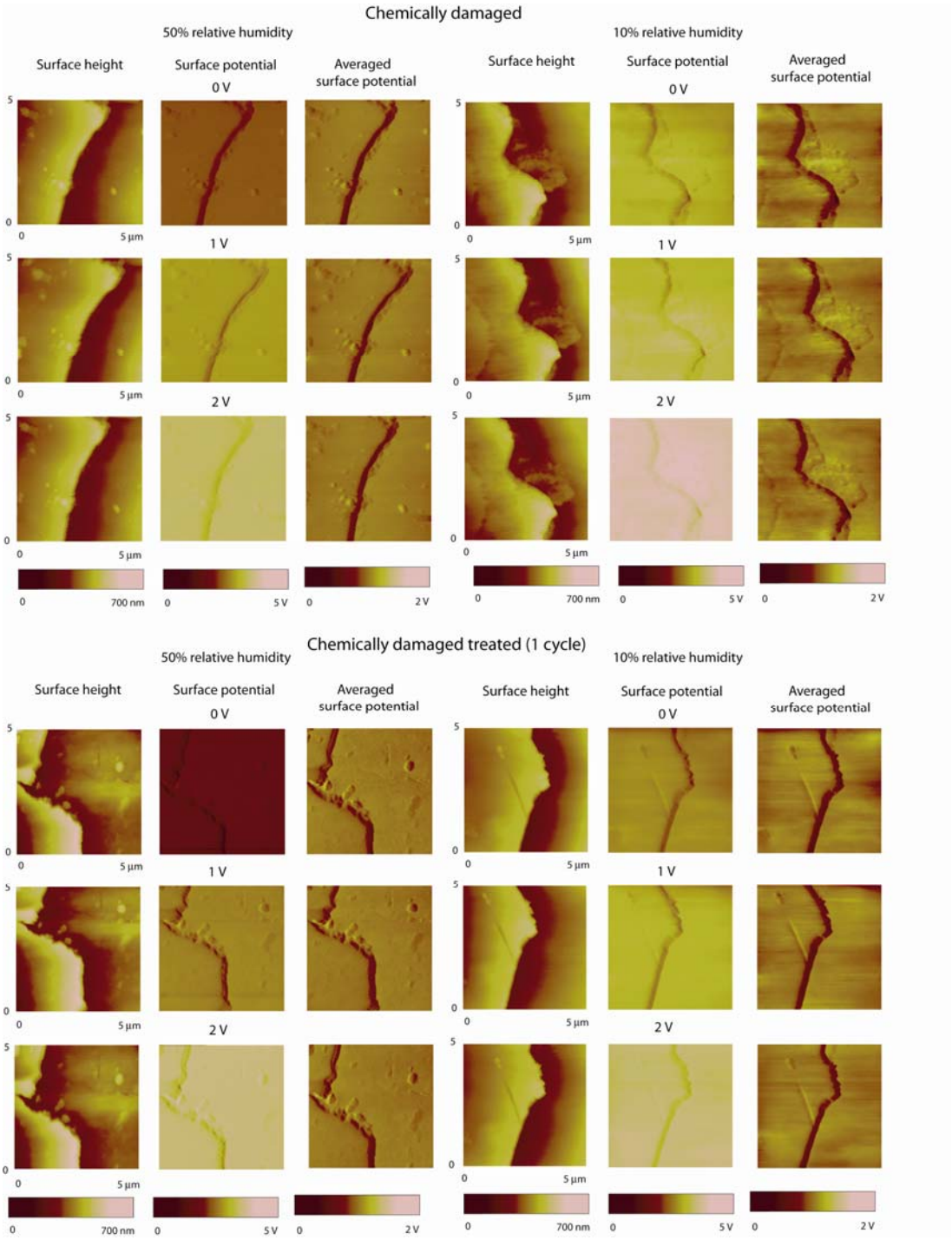

Figure 3.17 (continued)

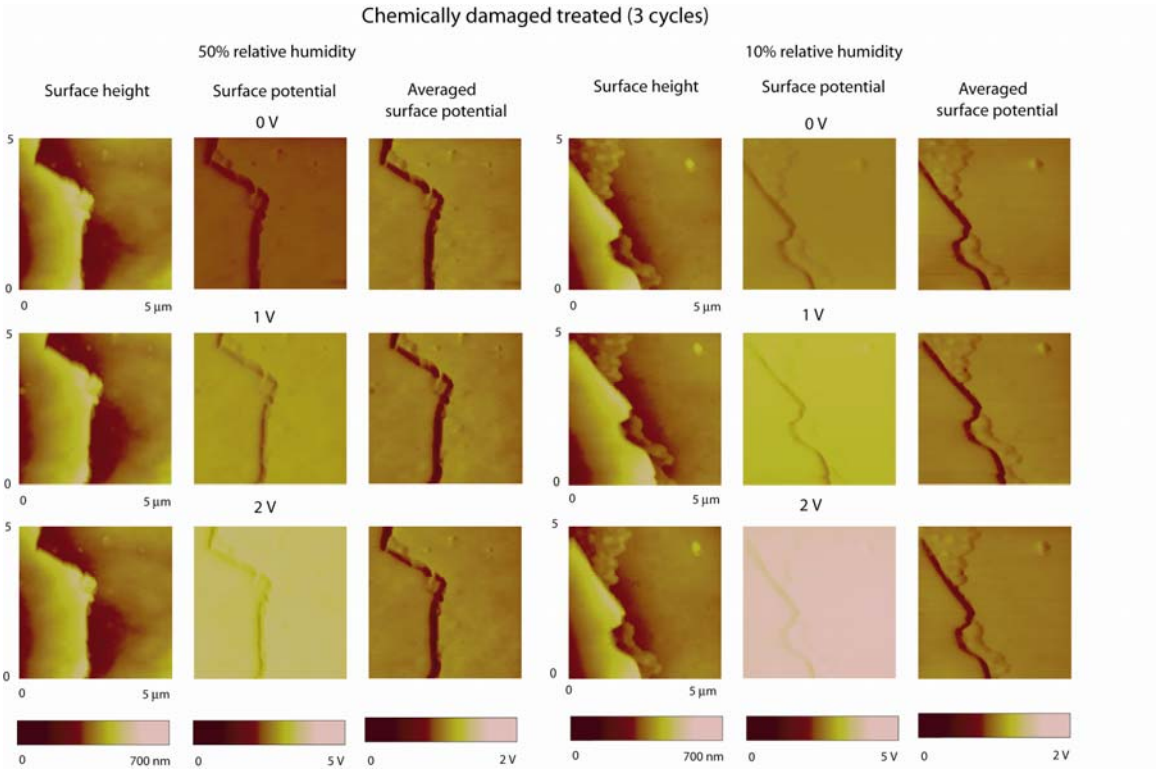

In this case, a higher 0-1 V value indicates more charge mobility and the ability to dissipate charge, whereas a lower value indicates less charge mobility. This being the case, it is evident that conditioner treatment greatly increases the mobility of surface charges. It is also shown that virgin hair has a better charge mobility and can therefore dissipate charge more readily than chemically damaged hair. This is likely due to the lipid layer that is intact in virgin hair, but has been removed in damaged hair.

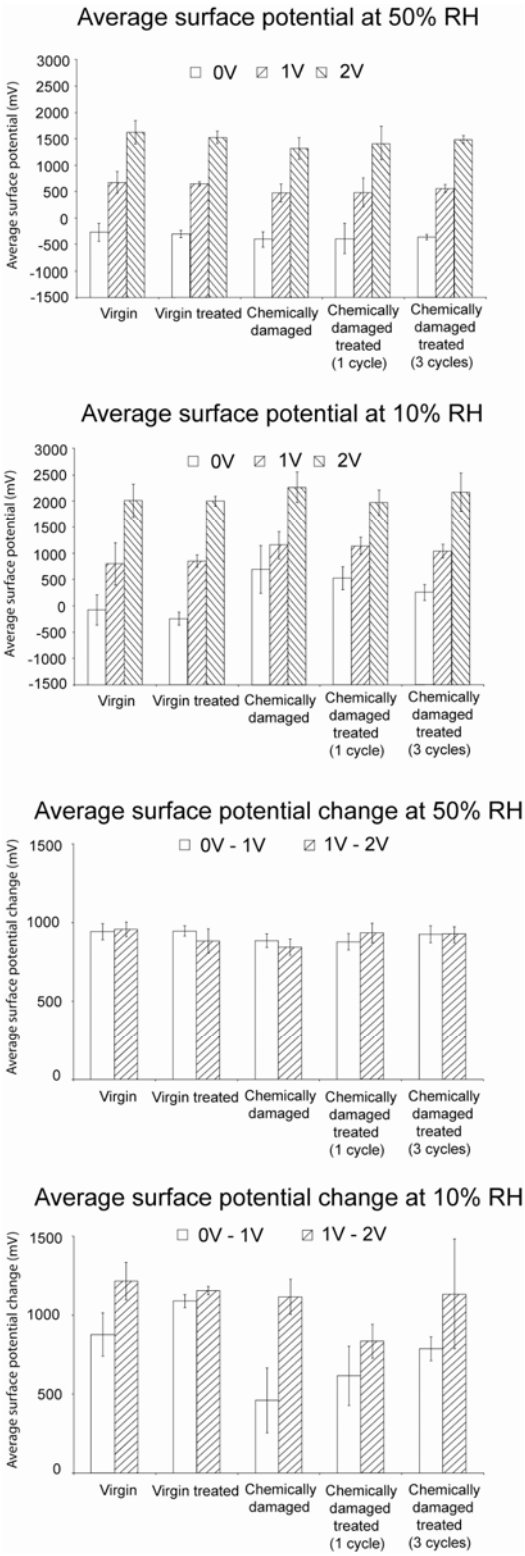

Figure 3.18 Bar charts showing average surface potential and average surface potential change at both 50% and 10% relative humidity.

Fig. 3.19 shows AFM images of chemically damaged hair treated with amino silicon conditioner. Here it is observed that the surface of the hair is more or less an equipotential surface, similar to the chemically damaged treated (3 cycles) sample . This suggests that the amino silicone conditioner coats the surface fully with one cycle, where commercial conditioner does not coat fully until several cycles.

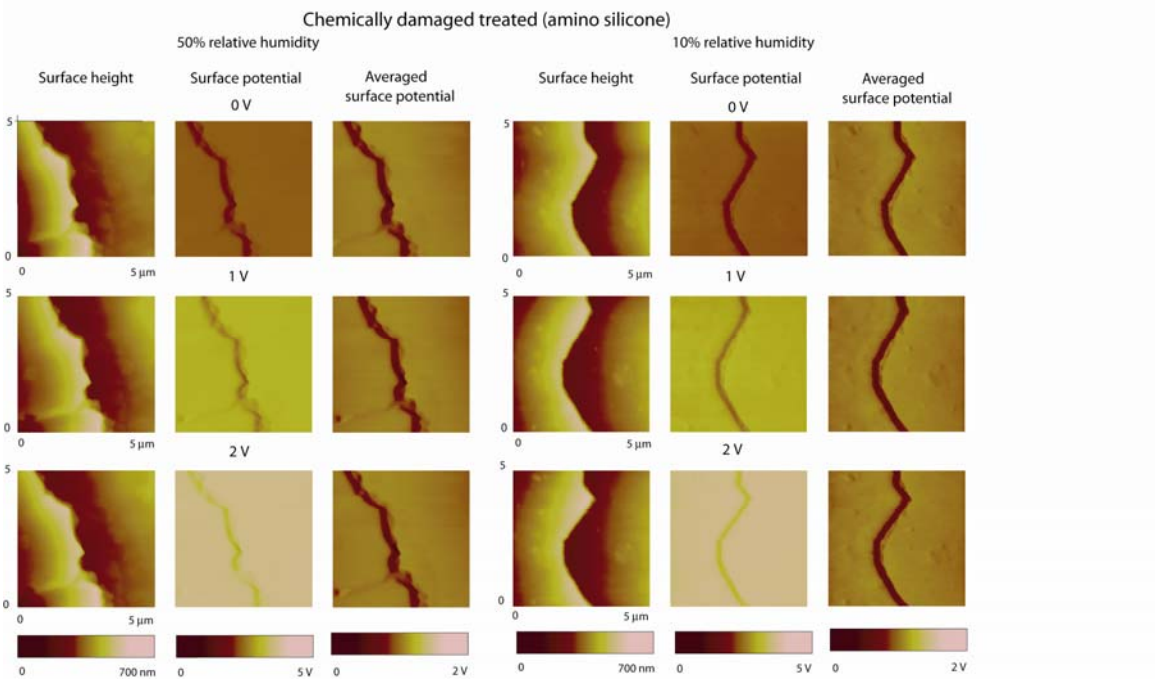

Figure 3.19 AFM images showing surface height and surface potential of chemically damaged treated (amino silicone) hair.

Fig. 3.20 shows this behavior as well. Amino silicone conditioner shows potential change in 10% relative humidity that are almost identical to those measured in 50% relative humidity. This indicates that the conditioner is evenly spread over the surface of the hair, which has been previously reported (LaTorre and Bhushan, 2006b; Lodge and Bhushan, 2006b). It also indicates that amino silicone conditioner

greatly increases charge mobility. Because commercial conditioner is unevenly distributed on the hair surface, the data for the commercially treated samples exhibit relatively high standard deviations in most cases. Consequently, different areas on the hair surface may contain vastly different amounts of conditioner on the surface. For the amino silicone case, however, different areas of the hair seem to have similar amounts of conditioner as evidenced by the lower standard deviation. The data then suggests that amino silicone conditioner is the superior conditioner in terms of charge dissipation.

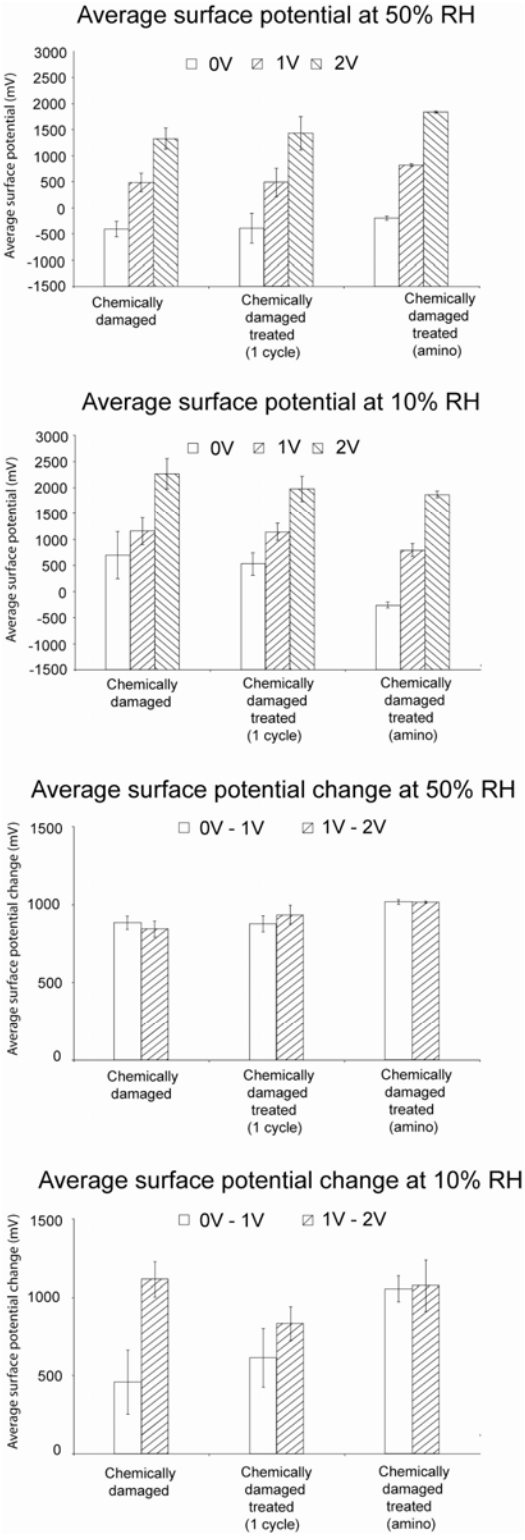

Figure 3.20 Bar charts showing average surface potential and average surface potential change at both 50% and 10% relative humidity.

3.5.1.3 Damage dependence

Fig. 3.21 shows AFM images of mechanically damaged hair. Here it is evident in the 10% relative humidity situation that trapped charges may exist near the scale edge. Because this sample experienced a high degree of cuticle damage, it is necessary that the cuticle edge came in contact with some object (comb, hand, etc.) that caused the damage. This interaction generally induces a triboelectric charge due to the contact of surfaces with very different electron affinities. If this is indeed the case for these samples, the areas of higher charge seen around the scale edges could easily be explained as occurring mechanically by triboelectric charging that happened during the creation of the mechanical damage. However, because these samples were not mechanically damaged in a controlled environment, much more work must be done on triboelectric effect before drawing definitive conclusions. It can also be seen from Fig. 3.22 that the mechanically damaged sample appears more closely related to virgin hair than chemically damaged. Again, this is because the mechanical damage occurs mostly at the scale edges, and the scale edges are neglected in this study due to the topography effect discussed earlier.

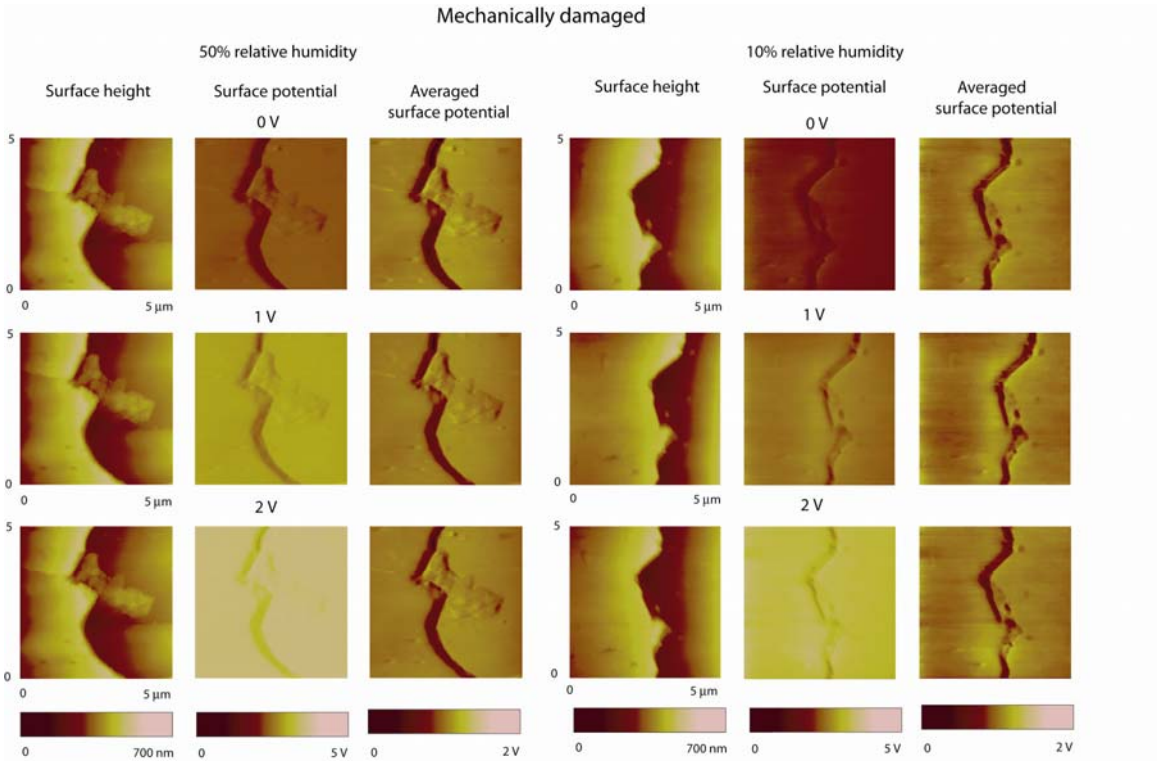

Figure 3.21 AFM images showing surface height and surface potential of mechanically damaged hair.

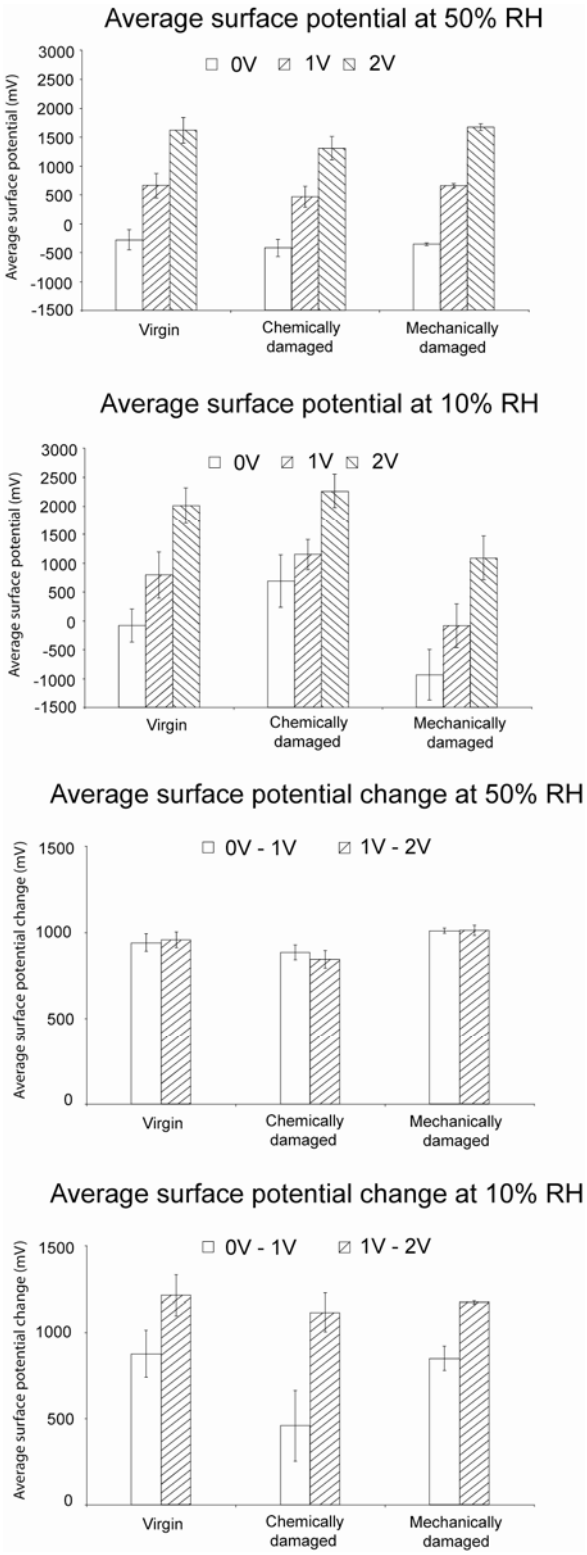

Figure 3.22 Bar charts showing average surface potential and average surface potential change at both 50% and 10% relative humidity.

3.5.2 Wear and triboelectric charging

3.5.2.1 Baseline materials

Results of wear tests on baseline samples are shown in Fig. 3.23. It is clear that the low load wear on the conductive aluminum sample, shown in Fig. 3.23(a), has a significant effect on the measured surface potential. Similar results are shown in DeVecchio and Bhushan (1998) and Bhushan and Goldade (2000a). The reason for such a change is well understood. The Kelvin probe method is physically measuring the contact potential difference between the tip and the sample. The contact potential difference is the difference in work functions of the tip and sample. The local work function is altered in the conducting sample because the physical wear alters the Fermi energy level locally, which is the kinetic energy of the most energetic electron at absolute zero. Thermodynamic equilibrium is destroyed by a change in Fermi level, and is reestablished in the material by a flow of electrons either to or from the worn area. This flow of electrons reestablishes equilibrium, which is the most stable state and will be maintained, but it also creates a change in work function due to the local excess or depletion of electrons. This excess or depletion results in a change in the measured surface potential. It is thus obvious that the migration of electrons through the material is critical for creating an area of different potential.

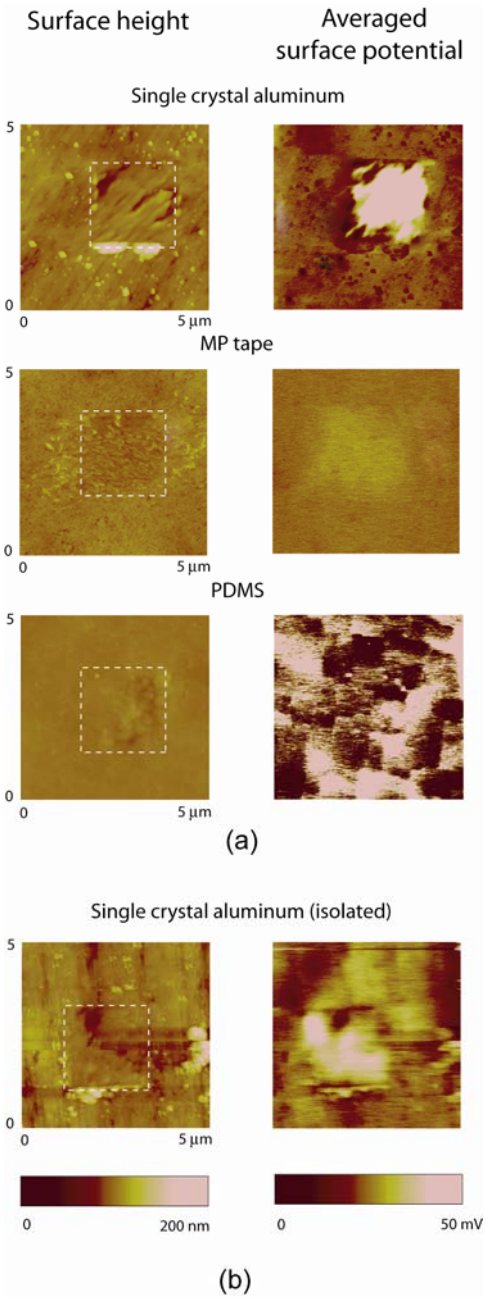

Figure 3.23 (a) AFM images showing base materials after making one pass with diamond tip at approximately 5 µN with sample grounded; (b) AFM image of single crystal aluminum after making one pass with diamond tip at 5 µN with sample electrically isolated from ground (dotted lines roughly show outline of wear scar on surface height map).

This mechanism is further confirmed in the MP tape and PDMS samples in Fig. 3.23(a), which show very little surface potential change which correlates with physical wear. The MP tape sample shown a very slight change which is expected because the metal particles in the tape are conductive and some migration of electrons through the sample may be possible because of this. However, this is not the case for PDMS, where it is clear that there is no correlation between the surface height map and the surface potential map. Electrons are not able to flow in this material, and thus no amount of wear will change the measured surface potential. Finally, the aluminum sample was isolated from ground and was again worn and then measured. It is evident that because the electrons in the metal sample are able to migrate, the surface potential is clearly affected by the wear. However, there is no sink for electrons to flow to without a ground connection, and the mobility of electrons is thus limited. This is shown in Fig. 3.23(b) where while there is a clear surface potential change in the area of wear, there are also areas of surface potential change that do not correlate to a wear mark. This is in contrast to the grounded aluminum sample in Fig. 3.23(a) which exhibited a more or less equipotential surface away from the wear scar.

The baseline materials indicate that a material must be conducting in order for physical wear to affect the local surface potential as measured with Kelvin probe microscopy. Further, the conducting sample must be grounded in order for a clear distinction to be made, in terms of surface potential, between the area affected by physical wear and the area which is not affected. The mobility of electrons within

and through the material is critical to this behavior. This indicates that physical wear is not the mechanism that causes surface potential change in insulating materials, such as human hair.

3.5.2.2 Hair samples

Fig. 3.24(a) shows AFM images for virgin and virgin treated hair samples. Chemically damaged, chemically damaged treated (1 cycle), and chemically damaged treated (3 cycles) samples are shown in Fig. 3.24(b). These images are presented in three columns. The first is the surface height of the sample and the second is the absolute surface potential. The final column shows the same surface potential data as the second column, but the average surface potential (which is presented in the subsequent bar charts) is subtracted out and the scale is reduced to show more contrast. It should be noted that some samples became highly charged as a result of the rubbing, beyond the capability of the microscope (10 V). These samples were not used. However, it is important to note that all of the samples tested are capable of developing high amounts of charge. A method where the force of contact is more accurately controlled may provide better insight into this behavior. Some samples, especially the chemically damaged one, show a significant amount of change in surface potential during measurement. This is illustrated as a higher potential at the bottom of the image than at the top, as the measurement was started at the bottom. This indicates that the charge dissipates relatively rapidly, and seems to reach a constant value by the time the measurement is finished. The fact that the virgin and treated samples seem to have a more constant potential during measurement indicates

that these samples dissipate charge faster, and by the time the measurement is taken a constant potential is more or less achieved. The average surface potential change is shown in Fig. 3.25. This bar chart indicates that conditioner treatment greatly reduces the amount of charge present on the hair surface. It also shows that chemical damage increases the amount of charge built on the hair surface. Similar results have been reported in previous studies (Lodge and Bhushan, 2006c).

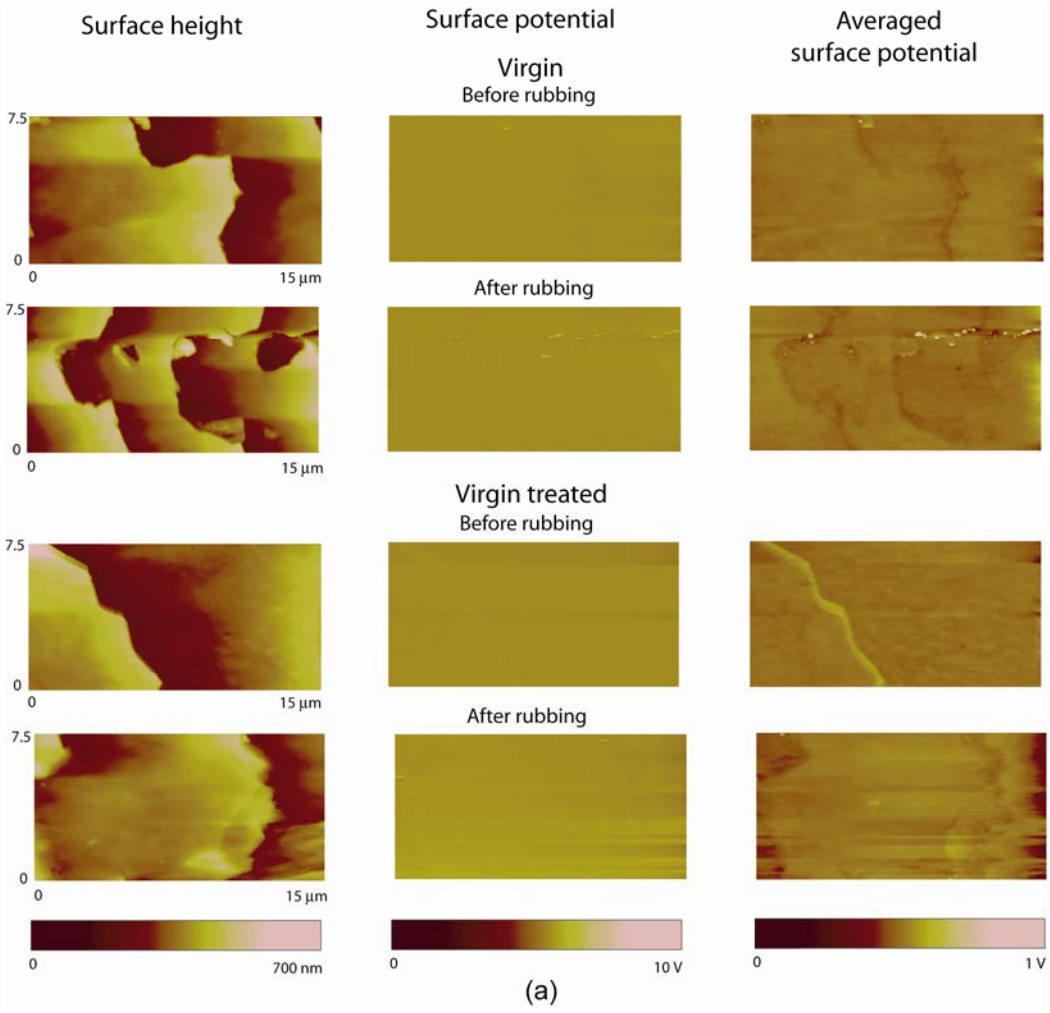

Figure 3.24 (a) AFM images of virgin and virgin treated hair samples both before and after rubbing with latex (b) Chemically damaged, chemically damaged treated (1 cycle), and chemically damaged treated (3 cycles) hair samples both before and after rubbing with latex. (continued on next page)

Figure 3.24 (continued)

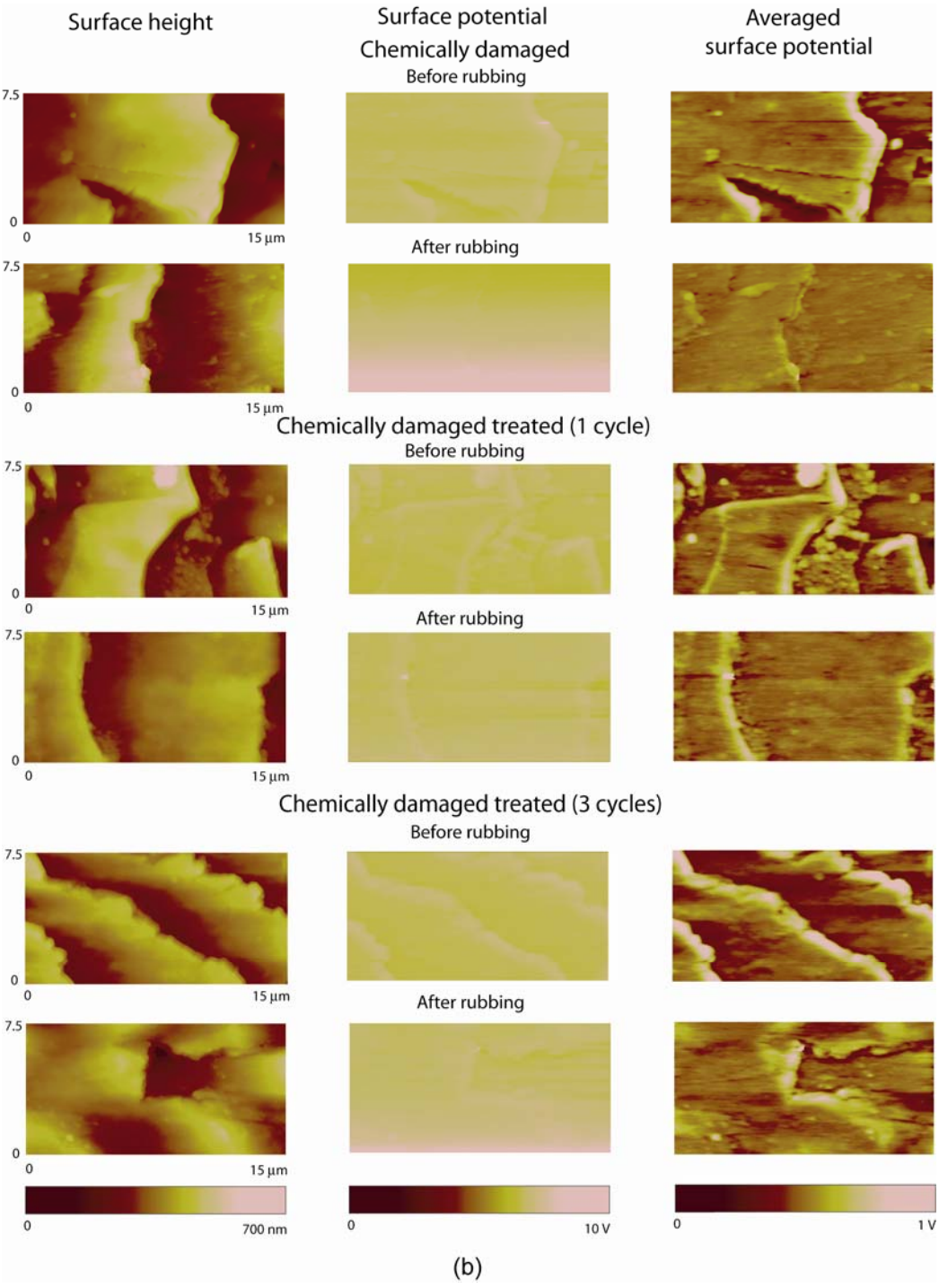

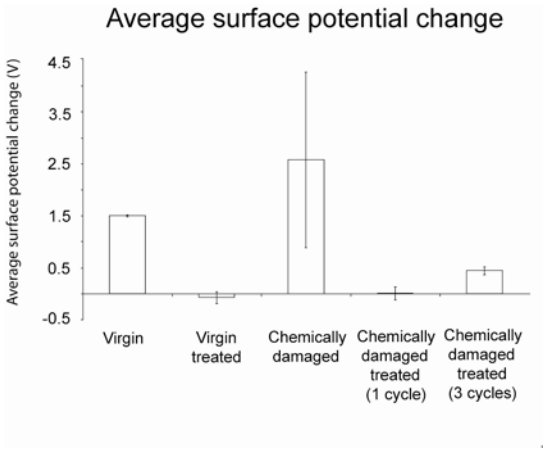

Figure 3.25 Bar chart of average surface potential change after rubbing with latex.

Fig. 3.26 shows chemically damaged hair that has been treated with a conditioner containing amino silicone, which is believed to chemically attach to the hair surface. Very little difference is seen between the amino silicone conditioner and the regular PDMS silicone conditioner. This is likely because the latex rubbing occurs over a very large area of the hair, and any difference in conditioner distribution is occurring on a much smaller scale. PDMS silicone conditioner is believed to only physically attach to the hair surface, and it remains mobile. Therefore, rubbing with the finger cot is likely to redistribute the conditioner, effectively spreading it evenly over the hair. However, amino silicone conditioner chemically attached to the surface, and distributes evenly to begin with. Moreover, amino silicone conditioner remains evenly distributed due to the chemical attachment. A method to rub the hair over a smaller area may provide more insight into this

behavior, and may elucidate the effect of conditioner distribution on surface potential properties. However, the amino silicone conditioner still shows a significant decrease in charge from the untreated chemically damaged sample.

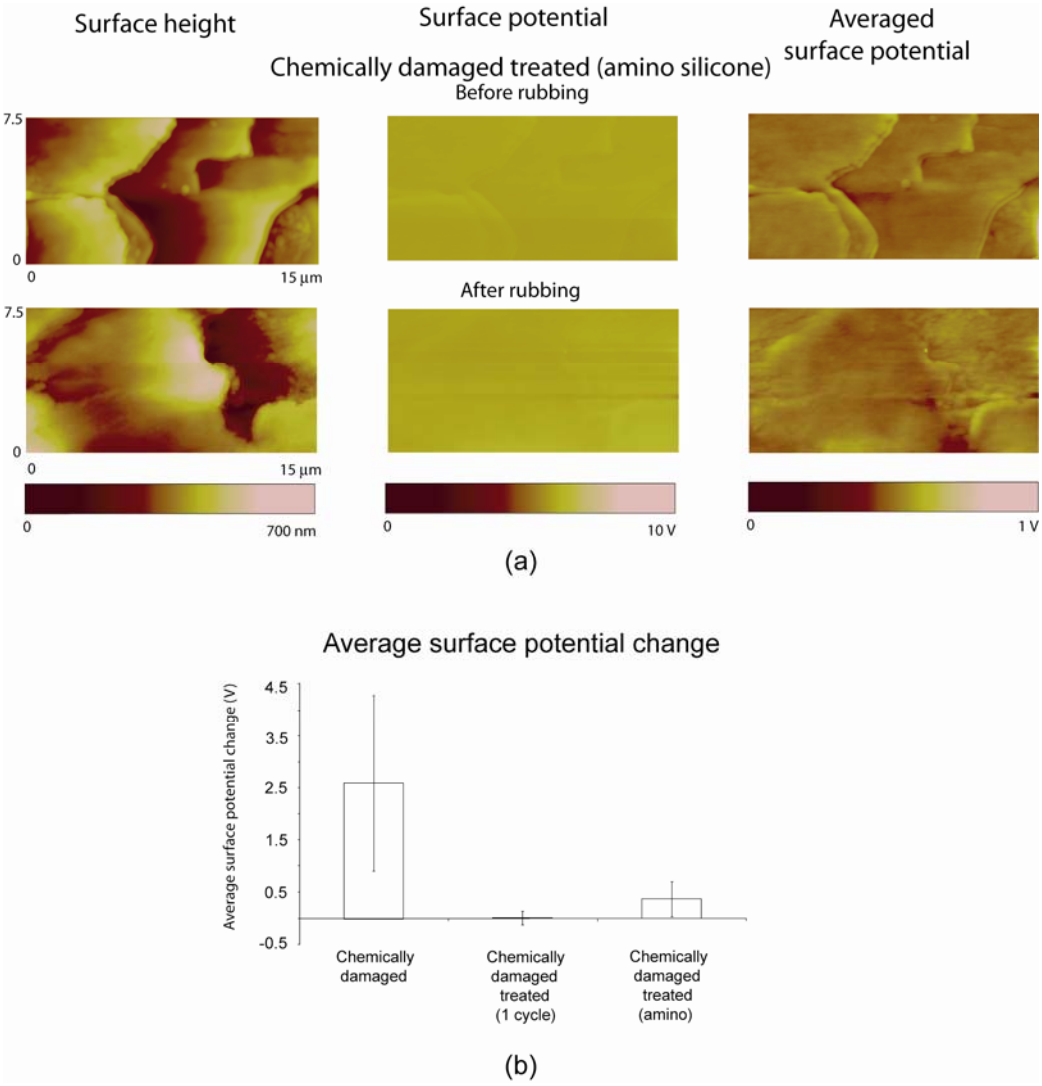

Figure 3.26 (a) AFM images of chemically damaged treated (amino) hair both before and after rubbing with latex; (b) Bar chart showing average surface potential change after rubbing with latex.

Fig. 3.27 shows mechanically damaged hair samples. This figure shows results more similar to virgin hair than to chemically damaged hair. This is likely due to the

fact that the top lipid layer of hair is not removed and that most of the mechanical damage occurs at scale edges. Chemical damage occurs over the entire surface of the hair. For this reason it is likely that mechanically damaged hair will behave more like virgin hair than chemically damaged hair. Because the rubbing procedure is not strictly controlled in terms of location of contact, it is difficult to distinguish a difference between the topmost layer of the hair, and the portions which have been mechanically damaged. However, this indifference between these regions (which generally occur on the surface away from scale edges, and near scale edges, respectively) may also be due to the fact that physical wear does not affect surface potential in insulating samples, as discussed previously.

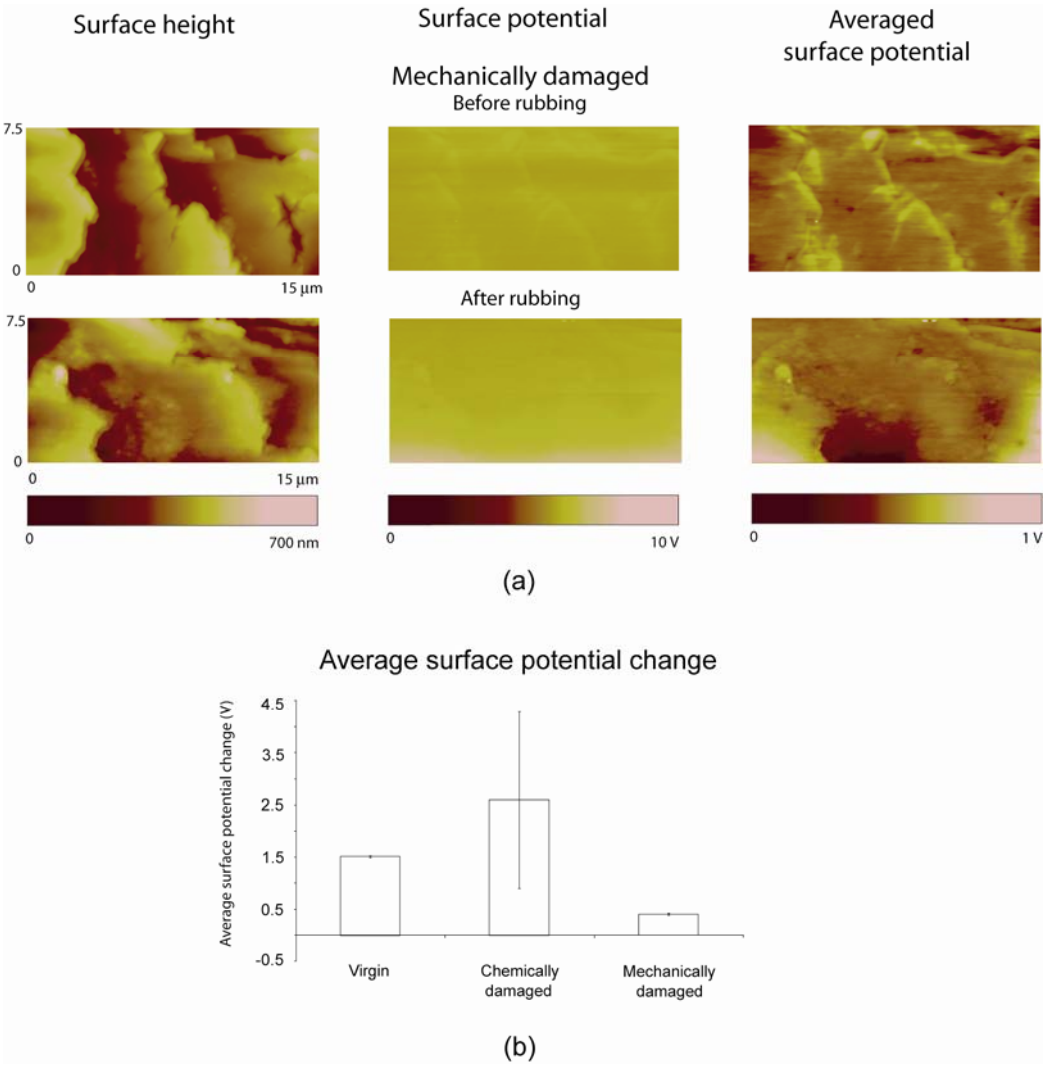

Figure 3.27 (a) AFM images of mechanically damaged hair both before and after rubbing with latex; (b) Bar chart showing average surface potential change after rubbing with latex.

CHAPTER 4

CONCLUSION

This thesis has presented a variety of results. New and existing measurement techniques have been applied to the science of hair care, and a number of new findings have resulted. Tapping mode was investigated as a method for imaging surface height of human hair as an alternative to contact mode, which had been used in previous studies. Additionally, the force calibration plot technique was used to map conditioner thickness distribution and adhesive force. The effect of hydrophobicity of the tip was also investigated by coating a silicon nitride tip with Z-TETRAOL. The wetting properties of hair were studied further by measuring the dynamic contact angle of various hairs by using the Wilhelmy balance method. Finally, the surface potential properties of human hair and other materials were investigated. The effect of wear on surface potential was studied and the mechanisms behind surface potential change as a result of physical wear were proven and discussed. The electrostatic charge on hair, which is a serious issue in the real world, was measured and studied by rubbing hair samples with a latex finger cot. The conclusions from the studies described in this thesis are quite varied, and constitute a firm foundation of understanding as well as a significant advancement from previous literature on the subject.

Tapping mode was found to be a much less destructive method for surface height imaging than contact mode. In general tapping mode is able to capture more high frequency information that contact mode due to its non-destructive nature. Additionally, tapping mode is capable of imaging actual conditioner deposits. Therefore, tapping mode is determined to be the more appropriate method for imaging all hair samples, and soft biological samples in general.

The snap-in distance H_s, derived from a force calibration plot, provides an accurate estimate of conditioner thickness on the hair surface. H_s is an overestimate of actual film thickness by 1-2 nm, but retains the correct trends. PDMS silicone conditioner unevenly distributes on the hair surface. Thickness increases with number of cycles of treatment, and the mean thickness varies from 4-6 nm, with local maxima approaching 25 nm in some instances. In additions to these findings, it was also found that the majority of conditioner that remains on hair after application deposits near the scale edge base. Here thicknesses up to 100 nm were found.

Coefficient of friction and adhesive force were measured with a Z-TETRAOL coated, hydrophobic AFM tip, and compared to values measured with an uncoated, hydrophilic tip. The results showed that meniscus forces contribute significantly to friction for hydrophilic surfaces, such as chemically damaged hair. Results also showed that the driving mechanism behind the increase in adhesive force with conditioner application is meniscus forces. This is a significant result due to the fact that the majority of earlier studies had used uncoated tips, and thus were affected by the meniscus force contribution.

The dynamic contact angle measurements of hair were obtained using the Wilhelmy balance technique, which was found to be a powerful tool in analyzing the wetting properties of thin fibers such as human hair. To study the contact angle of the surface of human hair away from cuticle scale edges where mechanical damage may alter results, the advancing direction using the against scale orientation is the most appropriate. Virgin hair was found to be hydrophobic as a result of the outer lipid layer coating its surface. Hair that has been damaged chemically or mechanically was found to be hydrophilic as a result of this outermost layer being at least partially removed during the damaging process. Conditioner treatment was found to lower the contact angle of virgin hair, and raise the contact angle of damaged hair. This effect of conditioner on the contact angle of the hair surface was found to explain the drastic drop in friction of damaged hair after conditioner treatment. The drop in friction is explained by a significant reduction in meniscus force contributions as a result of the increased contact angle of the hair surface. Finally, the large hysteresis values found in untreated samples is in contrast with the smaller hysteresis for treated samples. This indicates the presence of conditioner at the cuticle scale edge bases, which agrees with previous claims.

Kelvin probe microscopy was applied to human hair, and was found to be a powerful tool when used to study electrostatic properties of hair on the nano/micro scale. The technique is accurate and sensitive enough to visibly show areas of surface potential contrast on the hair surface. This was determined to be a result of physical or chemical differences on the surface, or locations of trapped charges. Relative humidity was found to play a significant role in the behavior of surface charges on

hair. A low relative humidity decreases charge mobility thereby increasing the likelihood of charges becoming trapped on the surface. In general, conditioner treatment increases charge mobility on the hair surface allowing easier charge dissipation regardless of the relative humidity. Amino silicone conditioner was found to coat the hair surface uniformly and provide higher charge mobility and less likelihood of trapped charges than the commercial conditioner studied. This is true even in low humidity conditions. This is the case because amino silicone conditioner chemically attaches to the hair surface, and thus provides a consistent, even coat on the hair that does not redistribute. This is in contrast to PDMS silicone conditioner which may not cover the entire hair surface, allowing the electrostatic properties of the underlying hair surface to dominate. Chemical damage is known to removes the natural lipid layer on virgin hair, and this was found to greatly decrease charge mobility on the surface. Therefore chemically damaged hair is more likely to develop and retain charge.

Because physical contact with other materials results in electrostatic charging of hair in the real world, physical wear was investigated as it relates to surface potential change. Physical wear is known to cause surface potential change in conducting materials due to the ability of electrons to flow through the material and establish thermodynamic equilibrium proceeding physical wear, and this was shown again in this thesis. However, because of the inability of electrons to flow through insulating materials, physical wear does not cause a change in surface potential in these materials. For this reason, physical wear alone can not cause an electrostatic charge on human hair because hair is non-conductive. Electrostatic charge on hair is

caused by introducing charges when a dissimilar material with a different electron affinity, such as latex, comes in contact with the hair. The resulting electrostatic charge can dissipate rapidly. The natural lipid layer on virgin hair and conditioner treatment may increase the rate of dissipation. Untreated chemically damaged hair, which has no lipid layer, seems to retain charge the longest. Finally, it was found that conditioner treatment significantly decreases the charge built on the hair surface by rubbing with a latex finger cot. This is true for both PDMS silicone conditioner as well as amino silicone conditioner.

LIST OF REFERENCES

A.H. Barber, S.R. Cohen, H.D. Wagner, "External and internal wetting of carbon nanotubes with organic liquids." *Phys. Rev. B* **71**, 115443 (2005).

B. Bhushan, *Principles and Applications of Tribology*, Wiley, New York, 1999a.

B. Bhushan (Ed.), *Handbook of Micro/Nanotribology*, CRC Press, Boca Raton, FL, 1999b.

B. Bhushan, *Introduction to Tribology*, Wiley, New York, 2002.

B. Bhushan (Ed.), *Springer Handbook of Nanotechnology*, Springer-Verlag, Heidelberg, Germany, 2004.

B. Bhushan and A. Goldade, "Kelvin probe microscopy measurements of surface potential change under wear at low loads" *Wear*, **244**, 104-117 (2000a).

B. Bhushan and A. Goldade, "Measurements and analysis of surface potential change during wear of single-crystal silicon (100) at ultralow loads using Kelvin probe microscopy" *Applied Surface Science*, **157**, 373-381 (2000b).

B. Bhushan, S. Sundararajan, W. W. Scott and S. Chilamakuri, "Stiction Analysis of Magnetic Tapes." *IEEE Trans. Mag.* **33** (1997) 3211-3213.

D. DeVecchio and B. Bhushan, "Use of a nanoscale Kelvin probe for detecting wear precursors" *Rev. Sci. Instrum.*, **69**, 3618-3624 (1998).

S. Ecke, M. Preuss, and H. Butt, "Microsphere Tensiometry to Measure Advancing and Receding Contact Angles on Individual Particles," *J. Adhesion Sci. Technol.* **13**, 1181-1191 (1999).

A. Efimov and S.R. Cohen, "Simulation and correction of geometric distortions in scanning Kelvin probe microscopy" *J. Vac. Sci. Technol. A*, **18**, 1051-1055 (2000).

A. Feughelman, *Mechanical Properties and Structure of Alpha-Keratin Fibres: Wool, Human Hair and Related Fibres*, University of South Wales Press, Sydney, 1997.

Ginn, M.E., Noyes, C.M., and Jungermann, E., "The Contact Angle of Water on Viable Human Skin", *J. of Colloid and Interface Sci.* **26** (1968) 146-151.

F. Hoecker, J. Karger-Kocsis, “Surface energetics of carbon fibers and its effects on the mechanical performance of CF/EP composites.” *J. App. Poly. Sci.* **59**, 139-153 (1996).

J. Jachowicz, G. Wis-Surel, M.L. Garcia, “Relationship between triboelectric charging and surface modifications of human hair” *J. Soc. Cosmet. Chem*, **36**, 189-212 (1985).

H.O. Jacobs, H.F. Knapp, A. Stemmer, “Practical aspects of Kelvin probe force microscopy” *Rev. Sci. Instrum.*, **70**, 1756-1760 (1999).

Y.K. Kamath, C.J. Dansizer, H.D. Weigman, “Wetting behavior of human hair fibers.”*J. Appl. Poly. Sci.* **22**, 2295-2306 (1978).

C.N.C. Lam, N. Kim, D. Hui. D.Y Kwok, M.L. Hair, A.W. Neumann, “The effect of liquid properties to contact angle hysteresis.”, *Coll. Surf. A Physico. Chem. Aspects* **189**, 265-278 (2001).

C. LaTorre and B. Bhushan, "Nanotribological characterization of human hair and skin using atomic force miscopy." *Ultramicroscopy*, **105** (2005a) 155-175.

C. LaTorre and B. Bhushan, "Nanotribological effects of hair care products and environment on human hair using atomic force microscopy." *J. Vac. Sci. Technol. A* **23** (2005b) 1034-1045.

LaTorre, C. and Bhushan, B. “Investigation of Scale Effects and Directionality Dependence on Adhesion and Friction of Human Hair Using AFM and Macroscale Friction Test Apparatus,” *Ultramicroscopy*, **106**, 720-734 (2006a).

C. LaTorre , B. Bhushan, J.Z. Yang, P.M. Torgerson, “Nanotribological effects of silicone type and deposition level and surfactant type on human hair using atomic force microscopy.” *J. Cosmetic Sci*., **57**, 37-56 (2006b).

D. R. Lide, Ed., *The CRC Handbook of Chemistry and Physics*, 85th ed. ,CRC Press, Boca Raton, 2004.

R.A. Lodge and B. Bhushan, “Surface characterization of human hair using tapping mode atomic force microscopy and measurement of conditioner thickness distribution”, *J. Vac. Sci. Tech. A*, **24**, 1258-1269 (2006a).

R.A. Lodge and B. Bhushan, “ Wetting properties of human hair by means of dynamic contact angle measurement” *J. App. Poly. Sci.* **102**, 5255-5265 (2006b).

A.C. Lunn and R.E. Evans, “The electrostatic properties of human hair” *J. Soc. Cosmet. Chem.*, **28**, 549-569 (1977).

C.M. Mills, V.C. Ester, H. Henkin, “Measurement of static charge on hair”, *J. Soc. Cosmet. Chem.*, **7**, 466-475 (1956).

R. Molina, F. Comelles, M. R. Julia and P. Erra, "Chemical modifications on human hair studied by means of contact angle determination." J. Colloid Interface Sci. 237 (2001) 40-46.

K. Morioka, *Hair Follicle – Differentiation Under the Electron Microscope*, Springer-Verlag, Tokyo, 2005.

C. Robbins, *Chemical and Physical Behavior of Human Hair 3rd Edition*, Springer-Verlag, New York, 1994.

A.P. Negri, H.J. Cornell, “A Model for the Surface of Keratin Fibers.” Textile Res. J. V.63 (1993) 109-115.

Schott H., “Contact Angles and Wettability of Human Skin”, *Journal of Pharmaceutical Sciences* **60** (1971) 1893-1895.

D.K. Schroder, *Semiconductor Material and Device Characterization*, 3rd Edition, Wiley, Hoboken, 2006.

J. A. Swift and J. R. Smith, "Atomic force microscopy of human hair." *Scanning,* **22** (2000) 310-318.

Tao, Z., and Bhushan, B. “Surface Modification of AFM Si_3N_4 Probes for Adhesion/Friction Reduction and Imaging Improvement”, *J. Phys. D: Appl. Phys.* **39** (2006) 3858-3862.

S. Timoshenko, *Strength of Materials Part 1 and Part 2*, 3rd Edition, Krieger, 1983.

Wei, G., Bhushan, B., and Torgerson, P. M., “Nanomechanical Characterization of Human Hair Using Nanoindentation and SEM,” *Ultramicroscopy* **105** (2005) 248-266.

L. Wilhelmy, “Ueber die Abhängigkeit der Capillaritäts-Constanten des Alkohols von Substanz und Gestalt des benetzten festen Körpers,” *Ann. Phys* **119**, 177-217 (1863).

C. Zviak (Ed.), *The Science of Hair Care*, Marcel Dekker, New York, 1986.

APPENDIX A. SHAMPOO AND CONDITIONER TREATMENT PROCEDURE

This appendix section outlines the steps involved in washing hair switches with shampoo and and/or conditioner.

- Shampoo treatments

Shampoo treatments consisted of applying a commercial shampoo evenly down a hair switch with a syringe. Hair was lathered for 30 seconds, rinsed with tap water for 30 seconds, then repeated. The amount of shampoo used for each hair switch was 0.1 cm^3 shampoo per gram of hair. Switches were hanged to dry in an environmentally controlled laboratory, and then wrapped in aluminum foil.

- Conditioner treatments

A commercial conditioner was applied 0.1cm^3 of conditioner per gram of hair. The conditioner was applied in a downward direction (scalp to tip) thoroughly throughout hair switch for 30 seconds, and then allowed to sit on hair for another 30 seconds. The switch was then rinsed thoroughly for 30 seconds. Switches were hanged to dry in an environmentally controlled laboratory, and then wrapped in aluminum foil.

APPENDIX B. CONDITIONER THICKNESS APPROXIMATION

We consider a cylindrical hair fiber of diameter D = 50 μm (radius R = 25 μm). For conditioner thickness calculations, the following assumptions are made: (1) hair and the material being added have the same density, (2) coating of material is uniform on the hair surface, (3) the cross-sectional area of a hair fiber remains constant along the longitudinal axis of the fiber (i.e. from root to tip); the hair fiber is perfectly cylindrical (circular cross-section), and (4) the deposited conditioner remains bonded to the cuticle surface (no absorption into the cuticle layer).

The cross-sectional area of an untreated hair fiber is initially calculated. By adding a specified amount of conditioner, this area will increase and cause the radius of the hair treated fiber to increase. This increase in the radius of the treated hair will be equivalent to the thickness of the conditioner layer. The original cross-sectional area A_c of hair fiber is

$$A_c = \pi R^2 = \pi\left(25\mu m\right)^2 = 1963.4954\mu m^2$$

Adding 200 ppm material to the surface (which is comparable to the amount that commercial conditioners typically deposit) will cause an increase in volume (for a unit fiber length) by 200 ppm, or by 0.0002. Thus, the cross -sectional area $A_{c,\ conditioner}$ of the treated hair will increase by the same amount to

$$A_{c,conditioner} = 1.0002 A_c = 1963.888\mu m^2$$

which results in a new radius $R_{conditioner}$,

$$R_{conditioner} = \sqrt{\frac{A_{c,conditioner}}{\pi}} = 25.0025\mu m$$

Therefore, subtracting the original radius from the radius after treatment increases the thickness of the hair by 0.0025 microns, or 2.5 nm.

It is important to note that the approximation of the conditioner thickness as 2.5 nm was determined for a particular hair diameter and material deposition amount (with the hair and material having equal densities). Although these are generally realistic approximations, hair diameter often varies by a factor of 2 and the deposition level can vary up to an order of magnitude. The conditioner layer has been shown to be non-uniform as well. Thus, actual conditioner thickness can deviate significantly from this number.